A FRACTIONALIZED QUANTUM SPIN HALL EFFECT

A MODEL FOR A FRACTIONALIZED QUANTUM SPIN HALL EFFECT

By

MICHAEL W. YOUNG, B.Sc.

A Thesis
Submitted to the School of Graduate Studies
in Partial Fulfillment of the Requirements
for the Degree
Master of Science

McMaster University

MASTER OF SCIENCE (2008)
(Physics)

McMaster University
Hamilton, Ontario

TITLE: A model for a Fractionalized Quantum Spin Hall Effect

AUTHOR: Michael W. Young, B.Sc.(University of Waterloo)

SUPERVISOR: Dr. Sung-Sik Lee, Dr. Catherine Kallin

NUMBER OF PAGES: ix, 68

Acknowledgements

I would like to thank my supervisors for constant guidance, patience, and wisdom during this project. My parents and family for constant encouragement in whatever I have chosen to do with my life. And last, but by no means least, Kate for being a source of many constants in my life. You are always there with constant support, constant smiles, and constant love.

Abstract

Effects of electron correlations on a two dimensional quantum spin Hall system are studied. We examine possible phases of a generalized Hubbard model on a bilayer honeycomb lattice with a spin-orbit coupling and short range electron-electron repulsions at half filling, based on the slave rotor mean-field theory. The phase diagram of the model is found for a special case where the interlayer Coulomb repulsion is comparable to the intralayer Coulomb repulsion.

Besides the conventional quantum spin Hall phase and a broken-symmetry insulating phase, we find a new phase, a fractionalized quantum spin Hall phase, where the quantum spin Hall effect arises for fractionalized spinons which carry only spin but not charge. Experimental manifestations of the exotic phase and effects of fluctuations beyond the saddle point approximation are also discussed.

We finally study a toy Bose-Hubbard model for the charge sector of the theory to gain some insight into the phase diagram away from the special Coulomb repulsion values.

Contents

List of Figures

Chapter 1

Introduction

The quantum spin Hall phase is a new state of matter which arises due to spin-orbit coupling in time reversal symmetric systems [1, 2]. It is characterized by a gap in the bulk and an odd number of Kramers pairs of gapless edge modes which are protected by a $\mathbb{Z}_2$ topological order [2–6]. The $\mathbb{Z}_2$ topological order here distinguishes time reversal symmetric states which have even and odd numbers of Kramers pairs, namely it is an integer which counts the number of edges states modulo 2. The quantum spin Hall effect has a $\mathbb{Z}_2$ number of 1, say, since there are an odd number of edge states, while a conventional band insulator may have an even number of edge states so the $\mathbb{Z}_2$ number is 0.

At low energies the quantum spin Hall state is described by an effective theory for the gapless edge states. Since time reversal symmetry is not broken the edge modes should be non-chiral; namely spin up propagates in one direction while spin down propagates in the opposite direction. Time reversal symmetry forbids back scattering between the left and right propagating modes within a single Kramers pair of edge states; such a term is odd under time reversal symmetry. Since these terms are forbidden, back scattering may not occur and the single edge modes will remain stable and gapless. However, if we have more than one Kramers pair single particle back scattering between different Kramers pairs is allowed. This back scattering will open a gap for the edge states. An even number of Kramers pairs are not robust and can be completely gapped out. On the other hand, an odd number of Kramers pairs has to have at least one gapless Kramers pair remaining. Therefore, when time reversal symmetry is present in the system the $\mathbb{Z}_2$ topological classification is robust. The different $\mathbb{Z}_2$ numbers imply that these two systems lie in different universality classes. Hence the quantum spin Hall phase is a new

type of "topological insulator".

The quantum spin Hall effect was first proposed to exist due to spin-orbit coupling in graphene at zero temperature [1]. However, hopes of observing this effect in graphene were quickly shown to be unrealistic due to the small spin-orbit gap. The spin-orbit coupling in graphene only creates a charge gap on the order of 10^{-3} meV [7], hence we would have to go to extremely low temperatures in order for thermal fluctuations to become negligible.

With graphene ruled out, the search was expanded to include other two dimensional materials. Bernevig *et al.* [8] showed that the same effect could be seen in the semi-conducting HgTe/(Hg,Cd)Te quantum wells. These specific quantum wells are zincblende-type semi-conductors. In these materials there are four bands which are relevant at the Fermi level [8], the electron-like conduction band which is made up of the two spin states of the s orbital, and the heavy hole-like valence band which is made up of the $|p_x + ip_y, \uparrow\rangle$ and $|-(p_x - ip_y), \downarrow\rangle$ orbitals. Within these four bands one can write down an effective Hamiltonian near the Γ point in the Brillouin zone that is nothing but two copies, one for each Kramers pair, of a massive Dirac Hamiltonian, with mass M. Here the "mass" is related to the energy gap between the s-like and p-like orbitals. Spin-orbit coupling is naturally included in this effective model through the $|p_x + ip_y, \uparrow\rangle$ and $|-(p_x - ip_y), \downarrow\rangle$ orbitals.

By adjusting the thickness of the HgTe section of the quantum well, d, one can tune the band structure of the well from a model with positive mass to a model with negative mass of the Dirac electron. When $d < d_c$, where d_c is a critical thickness, the system is a conventional semi-conductor with a positive mass, $M > 0$. However, when $d > d_c$ the band structure is given by the so-called "inverted" band structure where the s-like orbitals are lower than the p-like orbitals and the mass is negative, $M < 0$. Since the effective model has passed through a gapless point in the band structure the system has undergone a phase transition. This phase transition is a topological quantum phase transition that involves the transfer of a Chern number from one band to the other. This transfer of Chern number is identical to the phase transition that happens in massless graphene when spin-orbit coupling is added. Since the topology of the momentum space for the inverted semi-conductor quantum wells is the same as graphene with spin-orbit coupling we should expect the quantum spin Hall effect to appear here.

Recently experiments have been performed [9] on these quantum wells which clearly show evidence of the gapless edge states in the quantum spin Hall state. The quantum wells are set up in a six terminal Hall bar with varied thicknesses, a gate voltage is

applied in order to tune the Fermi energy. By tuning the Fermi energy one can drive the system into its insulating state by ensuring that the Fermi energy lies within the gap. Longitudinal resistance measurements in the inverted band regime revealed a residual conductance that is absent for the conventional semi-conducting regime. Upon varying the width of the Hall bar the same behavior is observed, indicating that the residual conductance arises due to the existence of edge channels.

The original model for the quantum spin Hall state [1] was proposed for non-interacting systems. However, it was later shown [10, 11] that the edge states are stable in the presence of weak time-reversal symmetric disorder or weak many-body interactions. This robustness of the edge states to interactions suggests that the topological order in the bulk is also robust against weak disorder [12] and interactions [13–15]. However, if the electron correlations become strong, a broken symmetry insulating phase, such as a dimer phase or an antiferromagnetic phase, may become stabilized. As a side remark we note that while the quantum spin Hall effect is known to arise due to spin-orbit coupling there has been recent work [16,17] suggesting that a quantum spin Hall effect may arise due to many-body interactions.

Other novel phases of matter that are of great interest are the fractionalized phases which arise due to electron-electron correlations. These phases are dubbed fractionalized phases due to the fact that the electron effectively splits up into separate parts which do not behave as an electron; the low energy excitations may carry only spin or charge, for example. The most well known example of this behavior is in the one dimensional Hubbard model where the low energy excitations are separate propagating spin and charge density waves. Another interesting class of fractionalized phases are "spin liquids" in $2+1$ dimensions which are phases where the spins remain disordered due to quantum fluctuations while the charge excitations are gapped [18–20]. Since the low energy excitations of the spin liquids are spinons which do not carry charge, these phases are fractionalized.

Spin liquids can be classified in terms of a mean-field ansatz associated with valence bond order parameters [21]. Beyond the mean-field approximation, the most important fluctuations are the phase fluctuations of the valence bond order parameters. Since this phase mode is covariantly coupled with spinons the low energy theory in a spin liquid phase becomes a gauge theory. While there are a myriad of possible gauge groups for spin liquid states, in this paper we will focus on the $U(1)$ spin liquid, where the phase fluctuation is described by a $U(1)$ gauge field.

Though there exists theoretical models which exhibit spin liquid ground states in $2+1$

D, currently there is no clear experimental evidence of their existence in nature. However, there is *some* experimental signatures that a spin liquid may exist in two dimensional frustrated magnets [22, 23].

Since either spin-orbit couplings or electron correlations can lead to exotic phases, it is interesting to ask what happens if both interactions become important. In this thesis we will address this question by examining the possibility that a new phase of matter may arise due to an interplay between spin-orbit coupling and electron-electron interactions. One possibility is a fractional quantum spin Hall state [2]. This fractional state corresponds to a time-reversal symmetric version of the fractional quantum Hall state. Here, we will consider an alternative possibility where the quantum spin Hall effect arises simultaneously with fractionalization in a spin liquid state. In order to study these effects, throughout this work we will use the honeycomb lattice since it is known to support both the quantum spin Hall state [1] and it may also support a spin liquid state [24, 25].

The outline of the this thesis is as follows: In the second chapter of this thesis we will derive a mean-field theory for an extended Hubbard model on a honeycomb lattice at a specific value of Coulomb interactions. After defining an ansatz for the order parameters of the mean-field theory we derive a system of self-consistent equations which give the ground state configuration of the order parameters. In the third chapter we will discuss the results obtained by solving the self-consistent equations and present the mean-field phase diagram of the Hubbard model, which contains a new fractionalized quantum spin Hall phase. Finally we write down the low energy theory of the novel phase. In chapter four we discuss the physical manifestations of the fractionalized phase. In chapter five we attempt to gain some insight into the behavior of the fractionalized phase away from the mean-field theory. Here we discuss the stability of the fractionalized phase against interactions and phase fluctuations of the mean-field order parameters. In chapter six we examine a toy model which we argue describes the charge sector of the extended Hubbard model when we do not assume any special values of Coulomb interactions.

Chapter 2

A Simple Hubbard Model for Fractionalization of the Quantum Spin Hall Effect

2.1 The Hamiltonian

The model that we choose to investigate the existence of a fractionalized quantum spin Hall effect has both spin-orbit coupling and electron-electron interactions on a honeycomb lattice. We begin by considering a bilayer honeycomb lattice system on a metallic substrate, Fig. 2.1. The necessity of the substrate and bilayer will be discussed in a moment. Each individual layer is described by a Hubbard Hamiltonian, and the two layers interact via short a ranged Coulomb term. The Hamiltonian takes the form

$$\begin{aligned} H = & - \sum_{(i,j)} \sum_{a,\sigma} \left(t_{ijaσ} c^{\dagger}_{iaσ} c_{jaσ} + h.c \right) - \sum_{ia} \mu_a \left(n_{ia} - 1 \right) \\ & + U \sum_{i,a} \left(n_{ia} - 1 \right)^2 + U' \sum_{i} \left(n_{i1} - 1 \right) \left(n_{i2} - 1 \right) \\ & - \sum_{ia} \mu_a \left(n_{ia} - 1 \right) \end{aligned} \tag{2.1}$$

where $n_{ia} = \sum_{\sigma} c^{\dagger}_{iaσ} c_{iaτ}$, $c_{iaσ}$ is the electron annihilation operator for site i, spin σ, layer $a = 1, 2$, U is the onsite intralayer interaction energy, and U' is the interlayer interaction energy which is only nonzero for sites directly above/below each other.

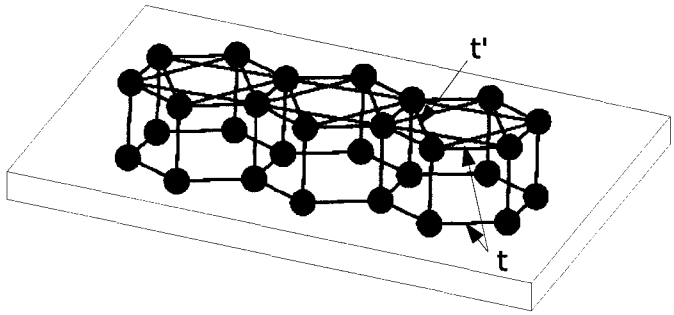

Figure 2.1: A bilayer honeycomb lattice on a metal substrate. The in-plane bonds between lattice sites represent the hopping integrals, t and t', while the interlayer bonds represent a short range Coulomb repulsion. In addition to interlayer Coulomb repulsion we also include onsite Coulomb repulsion within each layer. We denote the top layer as layer '1' and the bottom layer as layer '2'.

The hopping integral of the Hamiltonian above is defined by

$$t_{ija\sigma} = \begin{cases} t & ; \text{ if } (i,j) \text{ are nearest neighbours,} \\ t' e^{i\phi_{ij}\sigma}\delta_{a1} & ; \text{ if } (i,j) \text{ are next nearest neighbours.} \end{cases} \tag{2.2}$$

The next nearest neighbour hopping terms are analogous to those of Kane and Mele, Ref. [1], but differ in that we keep both the real and imaginary parts of the matrix element. However, keeping this real part only changes the band structure by an overall additive constant, not affecting the physics of the model. The spin dependent phase in the next nearest neighbour hopping integral is due to spin-orbit coupling. The origin of the phase can be understood as follows. From relativistic electromagnetism we know that a particle moving in a local electric field sees a magnetic field $\mathbf{B} = \frac{\mathbf{p}}{mc} \times \mathbf{E}$. If this particle is then allowed to have some spin we must add the Zeeman term $-\gamma\sigma \cdot \mathbf{B}$, where γ is a physical constant whose specific form is not important here, to the one body Hamiltonian which may be written as

$$-\gamma\sigma \cdot \mathbf{B} = -\gamma\sigma \cdot (\mathbf{p} \times \mathbf{E}) = -\gamma\mathbf{p} \cdot (\mathbf{E} \times \sigma) \ , \tag{2.3}$$

where we have absorbed the numerical factors that appear in the magnetic field into γ. With this new term the kinetic energy operator now becomes

$$\frac{\mathbf{p}^2}{2m} - \gamma\mathbf{p} \cdot (\mathbf{E} \times \sigma) \ . \tag{2.4}$$

With this new kinetic energy operator the hopping integral becomes

$$t_{ij} = \int_V \phi^*_{j\sigma} \left[-\frac{\nabla^2}{2m} + i\gamma \nabla \cdot (\mathbf{E} \times \sigma) \right] \phi_{i\sigma} = |t_{ij}| \, \mathrm{e}^{i\phi_{ij} \cdot \sigma} \, . \tag{2.5}$$

Although this spin dependent phase may appear in principle on both nearest neighbour *and* next nearest neighbour hopping integral terms, the nearest neighbour hopping terms in the honeycomb lattice do not contribute to the spin-orbit coupling that couples to S_z due to the lattice symmetry. The nearest neighbour hopping is taken to be isotropic, as in Ref. [24].

Now that we have discussed the origin of spin-orbit coupling on the honeycomb lattice

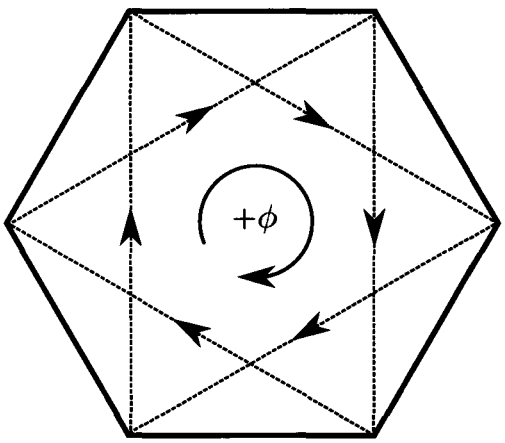

Figure 2.2: To assign the spin dependent phase we choose a convention that a spin up sees a positive phase if it hops around the lattice in a clockwise sense and a negative phase if it hops in the counter-clockwise sense. A spin down will see a positive phase if it hops in the counter-clockwise sense and a negative phase if it hops in a clockwise sense.

we may discuss the necessity of the double layer and the substrate. One key feature of the quantum spin Hall effect is the existence of a gap in the bulk. However, in order for a $U(1)$ spin liquid to be stable in $2+1$ dimensions we need to have gapless modes. This is due to the fact that the pure $U(1)$ gauge theory in $2+1$ D is always in its confining phase [26]. Hence in order to stabilize the fractionalized quantum spin Hall state with $U(1)$ guage symmetry, we need a second layer which provides these gapless modes.

The purpose of the substrate is to induce a system of image charges that will negate the effect of spin-orbit coupling on the second layer. The image charges will ensure that there is no tangential electric field in the plane of the second layer and thus the spin-orbit coupling term will not contribute to the hopping integral. When S_z is not conserved

there will be an additional Rashba spin-orbit coupling term. If this term becomes strong enough it may destabilize the quantum spin Hall state [1]. We will proceed under the assumption that if such a term exists it is small.

To describe a possible spin-charge separated phase we use the slave-rotor representation [27]. The slave-rotor representation is defined by the operator change of variables

$$c_{ia\sigma} = \mathrm{e}^{-i\theta_{ia}} f_{ia\sigma}, \tag{2.6}$$

where $\mathrm{e}^{-i\theta_{ia}}$ is the chargeon annihilation operator which destroys a chargeon particle that carries charge but no spin, and $f_{ia\sigma}$ is spinon annihilation operator which destroys a spinon particle that carries spin but no charge. Note, however, that we cannot just make this change of variables to the operators without any regard to the Hilbert space of the system. The representation (2.6) of the electron operators actually enlarges the Hilbert space of our original Hamiltonian [27]. This is because the chargeon can take values over an infinite set of integers, $\mathbb{Z}$, rather than the physical values, 0 and ± 1, where we the value '0' is for half filling. To project out these unphysical states we must introduce a constraint on the enlarged Hilbert space that will map us back to the physical Hilbert space.

To write down the constraint we notice that the chargeon operator, $\mathrm{e}^{-i\theta_{ia}}$, is a lowering operator of the charge quantum number. As such we can define a number operator L_{ia}, which is conjugate to θ_{ia}

$$[\theta_{ia}, L_{ib}] = i\delta_{ij}\delta_{ab} \ . \tag{2.7}$$

Since the charge on each site on a particular layer may only take on values 0 and ± 1 as stated above, we must constrain the charge quantum number per site to be ± 1 and 0 as well. We may do this by the constraint

$$L_{ia} = f^{\dagger}_{ia} f_{ia} - 1 \ . \tag{2.8}$$

We implement this constraint by a Lagrange multiplier, which must be added to the Hamiltonian as follows

$$ih_{ia}\left(\sum_{\sigma} f^{\dagger}_{ia\sigma} f_{ia\sigma} - 1 - L_{ia}\right) = 0, \tag{2.9}$$

The Hamiltonian in the slave-rotor representation is given by

$$H = -\sum_{\langle i,j\rangle}\sum_{a,\sigma}\left(t_{ija\sigma}f^{\dagger}_{ia\sigma}f_{ja\sigma}e^{i(\theta_{ia}-\theta_{ja})}+h.c\right)+U\sum_{ia}L^2_{ia}+U'\sum_{i}L_{i1}L_{i2}$$
$$+\ i\sum_{ia}h_{ia}\left(\sum_{\sigma}f^{\dagger}_{ia\sigma}f_{ja\sigma}-L_{ia}-1\right)-\sum_{ia}\mu_a\left(\sum_{\sigma}f^{\dagger}_{ia\sigma}f_{ja\sigma}-1\right)\ . \quad (2.10)$$

Our goal now is to find the mean-field phase diagram of this model.

2.2 Calculation of the Effective Action

In order to find the phase diagram of Hamiltonian (2.10) in terms of the chargeon and spinon degrees of freedom we need to find an effective action which governs both of these. To do this we compute the partition function within the functional integral representation

$$\mathcal{Z}=\int Df^*DfD\theta Dh e^{-S} \quad (2.11)$$

where S is the Euclidean action of the slave-rotor Hamiltonian after integrating out L_{ia}. We will treat each sector separately in order to minimize the intermediate formulae.

2.2.1 The Fermion Sector

We will first focus on the fermion sector of Hamiltonian (2.10). However, in the interest of generality we will consider an arbitrary fermionic Hamiltonian $H(\psi^{\dagger},\psi)$, which is a quadratic function of the fermionic fields ψ and $\psi^{\dagger}$. Our discussion in this section closely parallels that of Fradkin, Ref. [28]. We consider the partition function

$$\mathcal{Z}=\mathrm{Tr}\left[e^{-\beta(\hat{H}-\mu\hat{N})}\right]=\sum_{n}\langle n|e^{-\beta(\hat{H}-\mu\hat{N})}|n\rangle \quad (2.12)$$

where the states $|n\rangle$ form a complete set of states for the problem in question.

We can now compute the partition function

$$\begin{aligned}\mathcal{Z} &= \int d(\bar{\alpha},\alpha)\mathrm{e}^{-\sum_i \bar{\alpha}_i\alpha_i}\sum_n \langle n|\alpha\rangle\langle\alpha|\mathrm{e}^{-\beta(\hat{H}-\mu\hat{N})}|n\rangle \\ &= \int d(\bar{\alpha},\alpha)\mathrm{e}^{-\sum_i \bar{\alpha}_i\alpha_i}\sum_n \langle -\alpha|\mathrm{e}^{-\beta(\hat{H}-\mu\hat{N})}|n\rangle\langle n|\alpha\rangle \\ &= \int d(\bar{\alpha},\alpha)\mathrm{e}^{-\sum_i \bar{\alpha}_i\alpha_i}\langle -\alpha|\mathrm{e}^{-\beta(\hat{H}-\mu\hat{N})}|\alpha\rangle\end{aligned}$$

where the minus sign in the second line comes from the fermionic statistics when we switch the order of the inner products, and the integration measure is defined as $d(\bar{\alpha},\alpha) = \prod_{i=1}^{M} d\bar{\alpha}_i d\alpha_i$, for M the number of lattice sites. We now proceed by descretizing the 'time' interval $\beta = \epsilon/N$ which gives

$$\mathcal{Z} = \int_{BC's}\prod_{n=0}^{N} d(\bar{\alpha}^n,\alpha^n)\mathrm{e}^{-\epsilon\sum_{n=0}^{N-1}\left[\epsilon^{-1}(\bar{\alpha}^n-\bar{\alpha}^{n+1})\alpha^n + H(\bar{\alpha}^{n+1},\alpha^n)-\mu N(\bar{\alpha}^{n+1},\alpha^n)\right]} \tag{2.13}$$

where we have added a time-slice index to the Grassman variables. Now, if we take the limit $N\longrightarrow\infty$ and $\epsilon\longrightarrow 0$ we arrive at the action for the fermionic sector as

$$S[\bar{\psi},\psi] = \int_0^\beta d\tau\left(\bar{\psi}\partial_\tau\psi + H(\bar{\psi},\psi) - \mu N(\bar{\psi},\psi)\right) \tag{2.14}$$

where τ is the 'imaginary time'. This action is completely general and independent of the specific Hamiltonian in question. The fermion sector of our model is given by the terms in Eq. (2.10) that contain spinons.

2.2.2 The Boson Sector

The above procedure could be carried over into the bosonic sector in an analogous way, the only difference being the appearance of the minus sign and the coherent states used, but we will carry out a more detailed calculation here since our final intention is to integrate out L_{ia}. This will result in an action which contains only spinon and chargeon fiels. From hereon the L_{ia} sector of the Hamiltonian will be referred to as the 'charge sector'.

Since the charge sector of the Hamiltonian (2.10) is diagonal in site indices calculating

its partition function may be reduced to calculating one site matrix elements of the form

$$\mathcal{Z}_{i\theta} = \langle \theta_1' \theta_2' | \mathrm{e}^{-\epsilon H_L} | \theta_1 \theta_2 \rangle \tag{2.15}$$

where 1 and 2 refer to the layer index, $H_L = U(L_1^2 + L_2^2) + U' L_1 L_2 - i(h_1 L_1 + h_2 L_2)$, and a trace over the $|\theta\rangle$ states, which are coherent states of the operator θ_{ia} defined in appendix D, is understood to appear in the total partition function. Since the operators L_{ia} and θ_{ia} are conjugate to each other the overlap between the two bases is

$$\langle \theta' | l \rangle = \mathrm{e}^{il\theta'} \ . \tag{2.16}$$

Using this we can insert a complete set of number eigenstates, $|l\rangle$, on both layers to obtain

$$\mathcal{Z}_{i\theta} = \sum_{l_1, l_2} \mathrm{e}^{il_1(\theta_1' - \theta_1) + il_2(\theta_2' - \theta_2) - \epsilon \left[U(l_1^2 + l_2^2) + U' l_1 l_2 - i(h_1 l_1 + h_2 l_2) \right]} \ . \tag{2.17}$$

Now our goal is to integrate out all dependence on the variables l_{ia}. We do this by making a change of variables from the discrete l_{ia} to a new set of 'continuous' variables $p_a = \epsilon l_a$, in which case the sums in Eq. (2.17) become integrals and we have

$$\mathcal{Z}_{i\theta} = \frac{1}{\epsilon^2} \int dp_1 dp_2 \mathrm{e}^{ip_1 \left[\dot{\theta}_1 + h_1 \right] + ip_2 \left[\dot{\theta}_2 + h_2 \right] - \left[\frac{U}{\epsilon}(p_1^2 + p_2^2) + \frac{U'}{\epsilon} p_1 p_2 \right]}, \tag{2.18}$$

where

$$\frac{\theta_a' - \theta_a}{\epsilon} = \dot{\theta}_a, \tag{2.19}$$

which becomes the exact imaginary time derivative in the limit that $\epsilon \to 0$.

In order to perform these two integrals we change variables from p_1, p_2 to new variables

$$p_\pm \equiv \frac{1}{2}(p_1 \pm p_2) \tag{2.20}$$

which allow us to write the above coupled integrals as two decoupled Guassian integrals

$$\mathcal{Z}_{i\theta} = \frac{1}{2\epsilon^2} \int dp_+ dp_- \mathrm{e}^{2ip_+ \left[\dot{\theta}_+ + h_+ \right] + 2ip_- \left[\dot{\theta}_- + h_- \right] - \frac{1}{\epsilon} \left[(2U + U') p_+^2 + (2U - U') p_-^2 \right]} \tag{2.21}$$

where the factor of 2 is the Jacobian of the change of variables. It is convenient to define new coupling constants as $U_+ = 2U + U'$ and $U_- = 2U - U'$. We can now evaluate the

integrals to arrive at

$$\mathcal{Z}_{i\theta} = \frac{1}{2\epsilon^2}\sqrt{\frac{\pi\epsilon}{U_+}}\sqrt{\frac{\pi\epsilon}{U_-}}\, \mathrm{e}^{-\frac{\epsilon}{U_+}(\dot{\theta}_+ + h_+)^2} \mathrm{e}^{-\frac{\epsilon}{U_-}(\dot{\theta}_- + h_-)^2} \,. \tag{2.22}$$

Since this is the result for a single lattice point, the full angular partition function may be written as a product of the single site result above, which gives us the effective action for the chargeons (after going to the small ϵ limit) as

$$S_\theta = \int_0^\beta d\tau \left[\frac{1}{U_+} \sum_i \left(\dot{\theta}_{i+} + h_{i+} \right)^2 + \frac{1}{U_-} \sum_i \left(\dot{\theta}_{i-} + h_{i-} \right)^2 \right] \,. \tag{2.23}$$

The hopping sector of the action is easily obtained in the basis we are working in. Since the spinon operator does not affect the chargeon Hilbert space we can view this portion on the partition function as a direct product between two operators, one for the spinon space and the other for the chargeon space, for example $O_f \otimes O_\theta$. Thus the trace over the hopping sector of the Hamiltonian produces the same sum over neighbours only now the sum is number valued instead of operator valued.

Having obtained the effective actions for both spinon and chargeon sectors we now have the full action

$$\begin{aligned} S &= \int_0^\beta d\tau \left[\sum_{i,a,\sigma} f^*_{ia\sigma} \partial_\tau f_{ia\sigma} + \frac{1}{U_+} \sum_i (\partial_\tau \theta_{i+} + h_{i+})^2 + \frac{1}{U_-} \sum_i (\partial_\tau \theta_{i-} + h_{i-})^2 \right. \\ &- \left. \sum_{<i,j>,a,\sigma} \left(t_{ija\sigma} f^*_{ia\sigma} f_{ja\sigma} \mathrm{e}^{i(\theta_{ia} - \theta_{ja})} + h.c \right) + \sum_{i,a} (i h_{ia} - \mu_a) \left(\sum_\sigma f^*_{ia\sigma} f_{ia\sigma} - 1 \right) \right] \,. \end{aligned} \tag{2.24}$$

Due to the $U(1)$ phase redundancy this action is invariant under the local $U(1)$ gauge transformation

$$\begin{aligned} f_{ia\sigma} \rightarrow \mathrm{e}^{i\omega_i} f_{ia\sigma} \qquad & \theta_{i\pm} \rightarrow \theta_{i\pm} + \omega_i \\ h_{i\pm} \rightarrow & \; h_{i\pm} - \partial_\tau \omega_i \end{aligned} \tag{2.25}$$

2.3 The Special Case: $U' \approx 2U$

The effective action above is formally similar to that obtained in Ref. [24], the major difference being the doubled degrees of freedom due to the second layer. The appearance of the second boson field makes the problem more difficult. However, we can simplify the problem by considering a special case of the action (2.24) if we view it as two copies of a gauged anisotropic XY-model on a $3 = 2 + 1$ dimensional lattice.[1] The coupling in the temporal direction for each boson flavour is given by $1/U_\alpha$, $\alpha = \pm$, while the coupling in the 2 dimensional spacial lattice is given by the hopping parameters $t_{ij}\langle f^\dagger f\rangle$. If U' is small the temporal phase stiffness of the θ_{i-} field becomes very large.[2] This implies that the bosons will have a large, but finite, correlation length in the temporal direction, say ξ_τ.

Let us, for the moment, ignore the temporal component of the gauge field, $h_{i\alpha}$. Since the θ fields are correlated over a distance ξ_τ we may perform a coarse graining of the θ_{i-} fields into *block* phase degrees of freedom in the temporal direction. These block 'spins' then couple to each other with a strength proportional to the correlation length, ξ_τ, times the spacial coupling $t_{ij}\langle f^\dagger f\rangle$, since each spin within the block couples to a neighbouring spin in another block with strength $t_{ij}\langle f^\dagger f\rangle$. Thus as we tune U' closer to $2U$ the block θ_{i-}'s couple more and more strongly and thus they begin to become correlated over large distances in the spacial lattice as well. Since this effective block model for the bosons is 3 dimensional the continuous symmetry of the XY-model may be broken [29] and we can have a phase transition to a long range ordered phase, which in this case corresponds to the Bose condensed phase of the θ_{i-} field. When this is the case we may set $\theta_{i-} = 0$ which is equivalent to setting $\theta_{i1} = \theta_{i2}$ so our model reduces to a one boson model, which we may treat as in Ref. [24].

When we include the gauge field the condensation of the θ_{i-} boson gives a mass to the gauge field due to the Higgs mechanism. In the low energy theory the h_{i-} field may be integrated out to obtain an effective action for the remaining degrees of freedom.

[1] This viewpoint is justified in a later section where we decouple the spin and charge sectors through a Hubbard-Stratonovich transformation.

[2] Recall that the definitions above give $U_- = 0$ for $U' = 2U$.

The low energy action for the special case is

$$S = \int_0^\beta d\tau \left[\sum_{i,a,\sigma} f^*_{ia\sigma}\partial_\tau f_{ia\sigma} + \frac{1}{U_+}\sum_i (\partial_\tau\theta_i + h_{i+})^2 - \sum_{\substack{<i,j> \\ a,\sigma}} \left(t_{ija\sigma} f^*_{ia\sigma} f_{ja\sigma} e^{i(\theta_i-\theta_j)} + h.c\right) + \sum_{i,a}(ih_{ia} - \mu_a)\left(\sum_\sigma f^*_{ia\sigma} f_{ia\sigma} - 1\right)\right] . \tag{2.26}$$

Following Ref. [24] we introduce a soft boson field $X_i \equiv e^{-i\theta_i}$ subject to the constraint $|X_i| = 1$.[3] Rewriting the action we have

$$S = \int_0^\beta d\tau \left[\sum_{i,a,\sigma} f^*_{ia\sigma}\partial_\tau f_{ia\sigma} + \frac{1}{U_+}\sum_i [(i\partial_\tau + h_{i+})X^*_i][(-i\partial_\tau + h_{i+})X_i] - \sum_{\substack{<i,j> \\ a,\sigma}} \left(t_{ija\sigma} f^*_{ia\sigma} f_{ja\sigma} X_i X^*_j + h.c\right) + i\sum_i \lambda_i \left(|X_i|^2 - 1\right) + \sum_{i,a}(ih_{ia} - \mu_a)\left(\sum_\sigma f^*_{ia\sigma} f_{ia\sigma} - 1\right)\right] , \tag{2.27}$$

where we have added another Lagrange multiplier λ_i to enforce the soft boson constraint.

2.3.1 Hubbard-Stratonovich Transformation

The above action, Eq. (2.27), is quartic in hopping terms so we will perform a Hubbard-Stratonovich transformation, which will allow us to introduce mean-field order parameters. To do this we follow the method set forward in Ref. [24] and use the identity

$$\begin{aligned} e^{\epsilon\alpha\beta} &= \frac{\epsilon}{\pi}\int d\eta_R d\eta_I e^{-\epsilon\left[\eta_R - \frac{\alpha+\beta}{2}\right]^2 - \epsilon\left[\eta_I - i\frac{\alpha-\beta}{2}\right]^2 + \epsilon\alpha\beta} \\ &= \frac{\epsilon}{\pi}\int d\eta_R d\eta_I e^{-\epsilon\left[|\eta|^2 - \alpha(\eta_R + i\eta_I) - \beta(\eta_R - i\eta_I)\right]} \\ &= \frac{\epsilon}{\pi}\int d\eta_R d\eta_I e^{-\epsilon\left[|\eta|^2 - \alpha\eta - \beta\eta^*\right]} \\ &= \frac{-1}{2i}\frac{\epsilon}{\pi}\int d\eta d\eta^* e^{-\epsilon\left[|\eta|^2 - \alpha\eta - \beta\eta^*\right]} \end{aligned} \tag{2.28}$$

[3] The utility of this new field will become apparent when we compute the free energy of the boson sector.

where the factor of $-1/2i$ comes from the change of integration variables

$$\begin{aligned} d\eta \wedge d\eta^* &= (d\eta_R + i d\eta_I) \wedge (d\eta_R - i d\eta_I) \\ &= -i d\eta_R \wedge d\eta_I + i d\eta_I \wedge d\eta_R = -2i d\eta_R \wedge d\eta_I \ . \end{aligned} \tag{2.29}$$

We may now use this identity to transform the quartic hopping terms into quadratic form. The hopping Hamiltonian can be written as, neglecting the sums over layers and sites,

$$\sum_{(i,j)} H_{ij} = -t \sum_{(i,j)} (\alpha_{ij}\beta_{ij} + \alpha_{ji}\beta_{ji}) - t' \sum_{(i,k)} (\tilde{\alpha}_{ik}\beta_{ik} + \tilde{\alpha}_{ki}\beta_{ki}) \tag{2.30}$$

where $\alpha_{ij} \equiv \sum_{a,\sigma} f^*_{ia\sigma} f_{ja\sigma}$, $\tilde{\alpha}_{ik} \equiv \sum_{\sigma} e^{i\phi_{ik}\sigma} f^*_{i1\sigma} f_{k1\sigma}$, $\beta_{ij} \equiv X^*_j X_i$, and (i,j) are nearest neighbour pairs while (i,k) are next nearest neighbour pairs. Let us for the moment concentrate on the nearest neighbour hopping Hamiltonian. If we take only the nearest neighbour term for a specific time step, ε, we have

$$H_{\text{n.n.}} = -t(\alpha_{ij}\beta_{ij} + \alpha_{ji}\beta_{ji}) \ . \tag{2.31}$$

For each time step we may then use the identity (2.28) twice to write

$$\begin{aligned} e^{-\varepsilon H_{\text{n.n.}}} &= e^{\varepsilon t[\alpha_{ij}\beta_{ij} + \alpha_{ji}\beta_{ji}]} \\ &= \left(\frac{-1}{2i}\frac{\epsilon}{\pi}\right)^2 \int d\eta_{ij} d\eta^*_{ij} d\eta_{ji} d\eta^*_{ji} \\ &\qquad \times e^{-\epsilon\left[|\eta_{ij}|^2 + |\eta_{ji}|^2 - \alpha_{ij}\eta_{ij} - \alpha_{ji}\eta_{ji} - \beta_{ij}\eta^*_{ij} - \beta_{ji}\eta^*_{ji}\right]} \end{aligned} \tag{2.32}$$

where we have suppressed the τ dependence of the fields, in the second line we have set $\epsilon = \varepsilon t$, and introduced two sets of auxiliary fields to account for the Hermitian conjugate terms. To make the η variable manifestly complex, we let η take the form

$$\eta_{ij} = |\eta_{ij}| e^{i c_{ij}} \qquad\qquad \eta_{ji} = |\eta_{ji}| e^{i c_{ji}} \ . \tag{2.33}$$

The new integration measure can be computed by taking the exterior derivatives of (2.33) and evaluating their wedge products which gives

$$d\eta_{ij} \wedge d\eta^*_{ij} = -2i|\eta_{ij}| d|\eta_{ij}| \wedge dc_{ij} \ . \tag{2.34}$$

The new measure for η_{ji} can be obtained in the same fashion. With these changes the hopping integral becomes

$$\begin{aligned} e^{\varepsilon t[\alpha_{ij}\beta_{ij}+\alpha_{ji}\beta_{ji}]} &= \left(\frac{\epsilon}{\pi}\right)^2 \int d|\eta_{ij}|dc_{ij}d|\eta_{ji}|dc_{ji}|\eta_{ij}||\eta_{ji}| \\ & \quad e^{-\epsilon\left[|\eta_{ij}|^2+|\eta_{ji}|^2-\alpha_{ij}|\eta_{ij}|e^{ic_{ij}}-\alpha_{ji}|\eta_{ji}|e^{ic_{ji}}-\beta_{ij}|\eta_{ij}|e^{-ic_{ij}}-\beta_{ji}|\eta_{ji}|e^{-ic_{ji}}\right]} . \end{aligned} \tag{2.35}$$

We now make another change of variables to new fields[4]

$$\begin{aligned} |\eta_{ij}| &= |\chi_{ij}|e^{w_{ij}} & |\eta_{ji}| &= |\chi_{ij}|e^{-w_{ij}} \\ c_{ij} &= a_{ij}^+ + a_{ij} & c_{ji} &= a_{ij}^+ - a_{ij} \end{aligned} \tag{2.36}$$

which changes the measure to

$$d|\eta_{ij}|dc_{ij}d|\eta_{ji}|dc_{ji}|\eta_{ij}||\eta_{ji}| = 4|\chi_{ij}|^3 d|\chi_{ij}|dw_{ij}da_{ij}da_{ij}^+ . \tag{2.37}$$

Implementing this newest set of changes we have

$$\begin{aligned} e^{\epsilon[\alpha_{ij}\beta_{ij}+\alpha_{ji}\beta_{ji}]} &= 4\left(\frac{\epsilon}{\pi}\right)^2 \int d|\chi_{ij}|dw_{ij}da_{ij}da_{ij}^+|\chi_{ij}|^3 \\ & \quad \times\exp\Big\{-\epsilon\Big[2|\chi_{ij}|^2\cosh(2w_{ij}) - |\chi_{ij}|e^{ia_{ij}^+}\left(e^{w_{ij}+ia_{ij}}\alpha_{ij}\right. \\ & \qquad \left. + e^{-w_{ij}-ia_{ij}}\alpha_{ji}\right) \\ & \quad -|\chi_{ij}|e^{-ia_{ij}^+}\left(e^{w_{ij}-ia_{ij}}\beta_{ij} + e^{-w_{ij}+ia_{ij}}\beta_{ji}\right)\Big]\Big\} . \end{aligned} \tag{2.38}$$

Up to this point we have only treated the nearest neighbour hopping terms. However, we get the next nearest neighbour terms for free since we know the calculation will proceed in exactly the same manner, hence we will forgo an explicit calculation.

[4]This change of variables makes the definition of the mean-field order parameters to come more intuitive.

The full action for the hopping integral becomes

$$S_H = \int d\tau \Bigg\{ \sum_{\substack{<i,j> \\ a,\sigma}} t \Big[2|\chi_{ij}|^2 \cosh(2w_{ij}) - |\chi_{ij}| e^{ia^+_{ij}} \left(e^{w_{ij}+ia_{ij}} \alpha_{ij} + e^{-w_{ij}-ia_{ij}} \alpha_{ji} \right) - |\chi_{ij}| e^{-ia^+_{ij}} \left(e^{w_{ij}-ia_{ij}} \beta_{ij} + e^{-w_{ij}+ia_{ij}} \beta_{ji} \right) \Big] + \sum_{\substack{<<i,j>> \\ a,\sigma}} t' \Big[2|\tilde{\chi}_{ij}|^2 \cosh(2\tilde{w}_{ij}) - |\tilde{\chi}_{ij}| e^{\tilde{a}^+_{ij}} \left(e^{\tilde{w}_{ij}+i\tilde{a}_{ij}} \tilde{\alpha}_{ij} + e^{-\tilde{w}_{ij}-i\tilde{a}_{ij}} \tilde{\alpha}_{ji} \right) - |\tilde{\chi}_{ij}| e^{-i\tilde{a}^+_{ij}} \left(e^{\tilde{w}_{ij}-i\tilde{a}_{ij}} \beta_{ij} + e^{-\tilde{w}_{ij}+i\tilde{a}_{ij}} \beta_{ji} \right) \Big] \Bigg\}, \tag{2.39}$$

where the quantities with tildes represent the next nearest neighbour fields. The partition function will now involve an integral over all auxiliary fields, one for each nearest and next nearest neighbours, with integration measures given by Eq. (2.37).

2.3.2 Saddle Point Approximation and Mean-Field Order Parameters

Since we will focus on each sector individually we split the action up into three sectors

$$\begin{aligned} S^X = \int d\tau \Bigg[& \sum_i \frac{1}{U_+} \left(i\partial_\tau + h_{i+} \right) X^*_i \left(-i\partial_\tau + h_{i+} \right) X_i + i \sum_i \lambda_i |X_i|^2 \\ & - \sum_{<i,j>} t |\chi_{ij}| e^{-ia^+_{ij}} \left(e^{w_{ij}-ia_{ij}} X^*_j X_i + e^{-w_{ij}+ia_{ij}} X^*_i X_j \right) \\ & - \sum_{<<i,j>>} t' |\tilde{\chi}_{ij}| e^{-i\tilde{a}^+_{ij}} \left(e^{\tilde{w}_{ij}-i\tilde{a}_{ij}} X^*_j X_i + e^{-\tilde{w}_{ij}+i\tilde{a}_{ij}} X^*_i X_j \right) \Bigg], \end{aligned} \tag{2.40}$$

$$\begin{aligned} S^f = \int d\tau \Bigg[& \sum_{i,a,c} f^*_{ia\sigma} \left(\partial_\tau + i h_{ia} - \mu_a \right) f_{ia\sigma} \\ & - \sum_{\substack{<i,j> \\ a,\sigma}} t |\chi_{ij}| e^{ia^+_{ij}} \left(e^{w_{ij}+ia_{ij}} f^*_{ia\sigma} f_{ja\sigma} + e^{-w_{ij}-ia_{ij}} f^*_{ja\sigma} f_{ia\sigma} \right) \\ & - \sum_{<<i,j>>,\sigma} t' |\tilde{\chi}_{ij}| e^{i\tilde{a}^+_{ij}} \left(e^{\tilde{w}_{ij}+i\tilde{a}_{ij}} e^{i\phi_{ij\sigma}} f^*_{i1\sigma} f_{j1\sigma} + e^{-\tilde{w}_{ij}-i\tilde{a}_{ij}} e^{-i\phi_{ij\sigma}} f^*_{j1\sigma} f_{i1\sigma} \right) \Bigg], \end{aligned} \tag{2.41}$$

and

$$S^0 = \int d\tau \left[2 \sum_{<i,j>} t|\chi_{ij}|^2 \cosh(2w_{ij}) + 2 \sum_{<<i,j>>} t' |\tilde{\chi}_{ij}|^2 \cosh(2\tilde{w}_{ij}) + \sum_{ia} (\mu_a - i\lambda_i - ih_{ia}) \right] . \tag{2.42}$$

With the effective actions for each sector written in this form it is clear that there is a $U(1)$ gauge symmetry. The action $S = S^X + S^f + S^0$ is invariant under the $U(1)$ gauge transformations

$$f_{ia\sigma} \rightarrow f_{ia\sigma} e^{-i\omega_i} \qquad h_{ia} \rightarrow h_{ia} + \partial_\tau \omega_i \tag{2.43}$$

$$X_i \rightarrow X_i e^{-i\omega_i} \qquad a_{ij} \rightarrow a_{ij} - (\omega_i - \omega_j) \tag{2.44}$$

$$\tilde{a}_{ij} \rightarrow \tilde{a}_{ij} - (\omega_i - \omega_j) \tag{2.45}$$

Here h_i is the temporal component, and a_{ij} and $\tilde{a}_{ij}$ are the spatial components of the compact $U(1)$. Thus the bosons and fermions are coupled to each other through the $U(1)$ gauge field.

The above action has a bit of a problem, since it is not real. In order to make this action real we must make the analytical continuations

$$\begin{aligned} w_{ij} &= i\bar{w}_{ij} & a^+_{ij} &= i\bar{a}^+_{ij} \\ \lambda_i &= i\bar{\lambda}_i & h_i &= i\bar{h}_i \end{aligned} \tag{2.46}$$

where we have used Eq. (2.27) to state the continuations of the two Lagrange multipliers in the last line above. We will now ignore the fluctuations of these fields and let them take on their saddle point values, denoted above with an overbar on each field.

Upon carrying out the analytic continuation we have the boson sector written as

$$\begin{aligned} S^X = \int d\tau \Bigg[& \frac{1}{U_+} \sum_i [(i\partial_\tau + i\bar{h}_{i+})X_i^*][(-i\partial_\tau + i\bar{h}_{i+})X_i] - \sum_i \bar{\lambda}_i |X_i|^2 \\ & - \sum_{<i,j>} t \left(\chi_{ij}^{f\,*} X_j^* X_i + h.c. \right) - \sum_{<<i,j>>} t' \left(\tilde{\chi}_{ij}^{f*} X_j^* X_i + h.c. \right) \Bigg] \end{aligned} \tag{2.47}$$

where we have now defined the mean-field 'valence bond' order parameters $\chi^f_{ij} \equiv |\chi_{ij}| e^{\bar{a}^+_{ij} - i(\bar{w}_{ij} - \bar{a}_{ij})}$, and equivalently for the $\tilde{\chi}$ quantity.

We have the fermion sector as

$$S^f = \int d\tau \left[\sum_{i,a,\sigma} f^*_{ia\sigma} \left(\partial_\tau - \bar{h}_{ia} - \mu_a \right) f_{ia\sigma} - \sum_{\substack{<i,j> \\ a,\sigma}} t \left(\chi^X_{ij} f^*_{ia\sigma} f_{ja\sigma} + h.c. \right) \right.$$
$$\left. - \sum_{\substack{<<i,j>> \\ \sigma}} t' \left(\tilde{\chi}^X_{ij} e^{i\phi_{ij}\sigma} f^*_{i1\sigma} f_{j1\sigma} + h.c. \right) \right] \quad (2.48)$$

where $\chi^X_{ij} \equiv |\chi_{ij}| e^{-\bar{a}^+_{ij} + i(\bar{w}_{ij} + \bar{a}_{ij})}$, and equivalently for the $\tilde{\chi}$ quantity.

For the Lagrange multiplier sector we have

$$S^0 = \int d\tau \left[\sum_{<i,j>} t \left(\chi^{f*}_{ij} \chi^X_{ij} + h.c. \right) + \sum_{<<i,j>>} t' \left(\tilde{\chi}^{f*}_{ij} \tilde{\chi}^X_{ij} + h.c. \right) + \sum_{ia} \left(\mu_a + \bar{\lambda}_i + \bar{h}_{ia} \right) \right] . \quad (2.49)$$

2.4 The Ansatz

In this section we will describe the mean-field ansatze. We know that in the small U limit the two layers are decoupled with the first layer in the conventional quantum spin Hall phase and the second layer in the semi-metallic phase with two Fermi points where the quasiparticles have equal probability to move in any direction. This suggests that we should invoke a uniform ansatz for the valence bond order parameters, which represent hopping probabilities. In the large U limit the valence bonds fields are likely to be in a broken symmetry insulating phase and there is no conductivity. On a honeycomb lattice the simplest is the dimer ansatz. In both the uniform and dimer phases the electron density is uniform so we set the chemical potential on each layer to be site independant. We also take the Lagrange multipliers to be independent of site in both phases.

In order to justify our choice of a dimer ansatz in the large U limit it is helpful to use degenerate perturbation theory in t/U to obtain an effective Hamiltonian. In this section we will always assume that $U' = 2U$.

In the extremely large U case, where the hopping integrals may be neglected, the lowest energy states of the system are given by all states such that $\sum_a n_{ia} = 2$.[5] For a lattice with N sites this implies that there are 6^N degenerate low energy states. We may then apply perturbation theory to obtain an effective Hamiltonian that acts within this

[5]We see this result easily if we rewrite the original Hamiltonian, Eq. (2.1), as a complete square. The Coulomb terms will take the form $U \sum_i \left(\sum_a n_{ia} - 2 \right)^2$

degenerate manifold of states.

First we briefly review degenerate perturbation theory. Let $\{|l\rangle\}$ be a set of degenerate states of the Hamiltonian $H = H_0 + V$ with energy E, namely

$$H|l\rangle = E|l\rangle. \tag{2.50}$$

Let us assume that the perturbation V lifts all degeneracies so that we may split up the states $|l\rangle$ into its projections in and out of the degenerate space, namely we write $|l\rangle = \hat{P}_0|l\rangle + \hat{P}_1|l\rangle$. Here $\hat{P}$ is the projector onto the degenerate subspace and $\hat{P}_1 = 1 - \hat{P}_0$ is the projector out of the degenerate subspace. If we make this substitution into the Schrodinger equation (2.50) we may arrive at the effective Schrodinger equation in the low energy degenerate subspace

$$\left[(E - \varepsilon_0) - \hat{P}_0 V \hat{P}_1 \left(E - H_0 - \hat{P}_1 V \hat{P}_1\right)^{-1} \hat{P}_1 V \hat{P}_0\right] \hat{P}_0|l\rangle = 0, \tag{2.51}$$

where ε_0 is given by $H_0(\hat{P}_0|l\rangle) = \varepsilon_0(\hat{P}_0|l\rangle)$. The perturbation theory then comes in by choosing a small dimensionless parameter in which to use the matrix expansion

$$(\mathbb{A} - \mathbb{B})^{-1} = \left(1 + \mathbb{A}^{-1}\mathbb{B} + \mathbb{A}^{-1}\mathbb{B}\mathbb{A}^{-1}\mathbb{B} + ...\right)\mathbb{A}^{-1}. \tag{2.52}$$

For our particular case we will choose the perturbation operator to be the hopping term $T_{ij} = -t_{ija\sigma} c^\dagger_{ia\sigma} c_{ja\sigma}$ and the Coulomb term will be the unperturbed Hamiltonian. We then carry out the expansion for small hopping in terms of the dimensionless parameter t/U. Thus to first order in perturbation theory, for a two site problem, we arrive at the effective Hamiltonian

$$H_{\text{eff}}(ij) = \frac{1}{U} T_{ij} T_{ji}. \tag{2.53}$$

The total lattice Hamiltonian is then given by $H_{\text{eff}} = \sum_{(i,j)} H_{\text{eff}}(ij)$. With this general formula we can now simply write down the large U effective Hamiltonian of Eq. (2.1)

$$\begin{aligned} H_{\text{eff}} &= \frac{t^2}{U} \sum_{\substack{<i,j> \\ a,\sigma}} \left[c^\dagger_{ia\sigma} c_{ja\sigma} c^\dagger_{ja\sigma} c_{ia\sigma} + \text{h.c.}\right] \\ &+ \frac{t'^2}{U} \sum_{<<i,j>>} \left[e^{i\phi_{ij}\sigma^3} c^\dagger_{i1\sigma} c_{j1\sigma} e^{-i\phi_{ij}\sigma^3} c^\dagger_{j1\sigma} c_{i1\sigma} + \text{h.c.}\right]. \end{aligned} \tag{2.54}$$

The first term in (2.54) may be written in a $U(4)$ symmetric way be introducing the generators $[\mathcal{Q}_i]_{\alpha\beta} = c^\dagger_{i\alpha}c_{i\beta}$, where the indices α and β run over the four possible combinations of the layer (a) and spin (σ) index. While the second term may be written in a $U(2)$ symmetric way be introducing the generators $[\mathcal{T}_i]_{\sigma\sigma'} = c^\dagger_{i1\sigma}c_{i1\sigma'}$. The effective Hamiltonian can then be written, up to constant terms, in a more obviously symmetric way as

$$H_{\text{eff}} = \frac{t^2}{U}\sum_{<i,j>}\left(\text{Tr}\left[\mathcal{Q}_i\mathcal{Q}_j\right] + \text{h.c}\right) + \frac{t'^2}{U}\sum_{<<i,j>>}\left(\text{Tr}\left[e^{-i\phi_{ij}\sigma^3}\mathcal{T}_i e^{i\phi_{ij}\sigma^3}\mathcal{T}_j\right] + \text{h.c}\right). \quad (2.55)$$

The nearest neighbour term has a $U(4) = U(1)\otimes SU(4)$ symmetry, where the $U(1)$ symmetry represents total conservation of charge and the $SU(4)$ symmetry represents the conservation of flavour quantum number.[6] The next nearest neighbour term breaks this $U(4)$ symmetry into $SU(2)\otimes U(1)\otimes U(1)\otimes U(1)$. Here the unbroken $SU(2)$ represents spin rotation symmetry in the second layer and the three factors of $U(1)$ represent conservation of charge on each layer and S_z in the first layer.

The form of this effective Hamiltonian gives us some insight as to the proper ground state that we should choose. If $t' = 0$ the effective Hamiltonian describes an $SU(4)$ antiferromagnet, hence the nearest neighbour bonds will tend to form $SU(4)$ singlets which suggests that a valence bond solid is a good candidate for the ground state [30]. Of possible valence bond states on the honeycomb lattice the dimer phase is the most natural. When $t' \neq 0$ the dimer phase could potentially change into some other valence bond solid, but the dimer phase will remain stable for a finite range of $t' < t$.

In the figure below we illustrate the dimer ansatz. The uniform ansatz is obtained by letting the two distinct nearest neighbour couplings become equal and the two distinct next nearest neighbour couplings become equal.

Since our goal is to obtain a mean-field phase diagram for our model we must compute the free energy. To do this recall that the partition function is defined as

$$\mathcal{Z} = e^{-\beta_T F} \rightarrow F = \frac{-1}{\beta_T}\ln\mathcal{Z}\,. \quad (2.56)$$

Ignoring fluctuations of the order parameters the partition function is represented as

$$e^{-\beta_T F} = \int DfDf^*DXDX^* e^{-S}, \quad (2.57)$$

[6]Here the term 'flavour' refers to the combination of layer and spin indices.

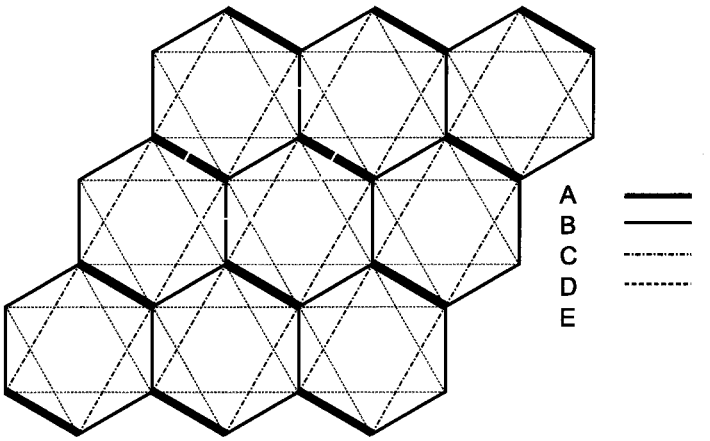

Figure 2.3: The dimer ansatz on the honeycomb lattice. The line segments represent the following: $\mathbf{A}$: $\chi^f_{\mathbf{J}BJA} \rightarrow \chi^f_1$, $\mathbf{B}$: $\chi^f_{(\mathbf{J}+a_2)BJA} \rightarrow \chi^f_2$, $\mathbf{C}$: $\chi^f_{(\mathbf{J}+\mathbf{a}_1+\mathbf{a}_2)\alpha\mathbf{J}\alpha} \rightarrow \chi'^f_1$, while $\mathbf{D}$ represents the other next nearest neighbour bonds, χ'^f_2. The superscript f here indicates that these are the fermion order parameters. The valence bonds will have the same form for the bosons but they will contain the superscript 'X'. The line segment $\mathbf{E}$ is the unit cell of the honeycomb lattice.

where $S = S^0 + S^f + S^X$. Thus we may calculate the mean-field free energy of each sector by evaluating the path integrals in

$$F = \frac{-1}{\beta_T} \ln \left[\int DfDf^* DXDX^* \mathrm{e}^{-S} \right] . \tag{2.58}$$

Since our effective action is broken up into the three sectors, Eqs. (2.47), (2.48), and (2.49), our free energy may also be computed sector by sector. For the Lagrange multiplier sector this turns out to be very simple, since it does not have any boson or fermion field dependence so we don't have to worry about any integrals. Thus at the saddle point we have

$$\begin{aligned} F^0 &= \frac{1}{\beta_T} \int_0^{\beta_T} d\tau \left\{ \sum_{<i,j>} t \left[\chi^{f\,*}_{ij} \chi^X_{ij} + h.c. \right] + \sum_{<<i,j>>} t' \left[\tilde{\chi}^{f*}_{ij} \tilde{\chi}^X_{ij} + h.c. \right] \right. \\ &\qquad \left. + \sum_{ia} \left(\mu_a + \bar{\lambda}_i + \bar{h}_{ia} \right) \right\} \\ &= \left\{ \sum_{<i,j>} t \left[\chi^{f\,*}_{ij} \chi^X_{ij} + h.c. \right] + \sum_{<<i,j>>} t' \left[\tilde{\chi}^{f*}_{ij} \tilde{\chi}^X_{ij} + h.c. \right] + \sum_{ia} \left(\mu_a + \bar{\lambda}_i + \bar{h}_{ia} \right) \right\} , \end{aligned} \tag{2.59}$$

where we ignore fluctuations of the order parameters.

To calculate the bosonic free energy we transform to momentum space, in which the action becomes diagonal. Since the honeycomb lattice has two sites per unit cell the energy spectrum should have two bands (eight for fermions due to the spin and layer indices). To account for multiple bands we write the fields as

$$X_i = X_{Is} \equiv \frac{1}{\sqrt{N\beta_T}} \sum_{\mathbf{k},\omega} \mathrm{e}^{-i\omega\tau + i\mathbf{k}\cdot\mathbf{I}} X_s(\mathbf{k},\omega), \tag{2.60}$$

where the vector $\mathbf{I}$ represents the unit cell position vector, and s is the site within the unit cell. Fourier transforming the boson sector we have

$$\begin{aligned} S^X = \Bigg\{ & \frac{1}{U_+ N} \sum_{\mathbf{I},s} \sum_{\substack{\mathbf{k},\mathbf{k}' \\ \omega}} [-\omega + i\bar{h}_{\mathbf{I}s+}]^2 \mathrm{e}^{i(\mathbf{k}-\mathbf{k}')\cdot\mathbf{I}} X_s^*(\mathbf{k}',\omega) X_s(\mathbf{k},\omega) \\ & - \frac{1}{N} \sum_{\mathbf{I},s}{}' \sum_{\substack{\mathbf{k},\mathbf{k}' \\ \omega}} \bar{\lambda}_{\mathbf{I}s} \mathrm{e}^{i(\mathbf{k}-\mathbf{k}')\cdot\mathbf{I}} X_s^*(\mathbf{k}',\omega) X_s(\mathbf{k},\omega) + \sum_{\substack{\mathbf{k},\omega \\ s}} \mathrm{e}_s^X(\mathbf{k}) |X_s(\mathbf{k},\omega)|^2 \Bigg\} . \end{aligned} \tag{2.61}$$

Here $\mathrm{e}_s^X(\mathbf{k}) = -t'\Gamma_{\mathbf{k}}^f + st\sqrt{|\Omega_{\mathbf{k}}^f|^2}$ is the energy spectrum of the bosons with

$$\Omega_{\mathbf{k}}^f \equiv \chi_1^f + \chi_2^f \left(\mathrm{e}^{-i\mathbf{k}\cdot\mathbf{a}_2} + \mathrm{e}^{i\mathbf{k}\cdot\mathbf{a}_1} \right) \tag{2.62}$$

and

$$\Gamma_{\mathbf{k}}^f \equiv 2 \left(\chi^{f'}{}_1 \cos[\mathbf{k}\cdot(\mathbf{a}_1+\mathbf{a}_2)] + \chi^{f'}{}_2 [\cos(\mathbf{k}\cdot\mathbf{a}_2) + \cos(\mathbf{k}\cdot\mathbf{a}_1)] \right) . \tag{2.63}$$

In the following we will focus on the uniform ansatz in which case the two Lagrange multipliers do not have any site or unit cell dependence. The we can bring them outside of the sums, in which case we would pick up a delta function in momentum which would make the momentum space action diagonal. Once we make this choice we can write the above action in a completely diagonal form as

$$S^X = \sum_{\substack{\mathbf{k},\omega \\ s}} \left\{ \frac{1}{U_+} [-\omega + i\bar{h}_+]^2 - \bar{\lambda} + \mathrm{e}_s^X(\mathbf{k}) \right\} |X_s(\mathbf{k},\omega)|^2 . \tag{2.64}$$

Thus the boson sector free energy is obtained by evaluating

$$F^X = -\frac{1}{\beta_T} \ln \left[\int DXDX^* \mathrm{e}^{-\sum_{\mathbf{k},\omega \atop s} \left\{ \frac{1}{U_+}[-\omega + i\bar{h}_+]^2 - \bar{\lambda} + \mathrm{e}_s^X(\mathbf{k}) \right\} |X_s(\mathbf{k},\omega)|^2} \right] . \tag{2.65}$$

The integral is now quadratic and we can perform the bosonic path integral easily; see for example pages 157-194 of Ref. [31]. The result is

$$F^X = \frac{1}{\beta_T} \sum_{\mathbf{k},\omega \atop s} \ln \left[\frac{1}{U_+}[-\omega + i\bar{h}_+]^2 - \bar{\lambda} + \mathrm{e}_s^X(\mathbf{k}) \right] . \tag{2.66}$$

Since we are interested in $T = 0$ behavior we replace the Matsubara summation with an integral,

$$\frac{1}{\beta_T} \sum_{\omega} \rightarrow \int \frac{d\omega}{2\pi} \tag{2.67}$$

which gives

$$E^X = \sum_{\mathbf{k},s} \int \frac{d\omega}{2\pi} \left\{ \ln \left[[-\omega + i\bar{h}_+]^2 + U_+(-\bar{\lambda} + \mathrm{e}_s^X(\mathbf{k})) \right] - \ln U_+ \right\} . \tag{2.68}$$

We can perform this integral by using the integral identity

$$\int \frac{d\omega}{2\pi} \left\{ \ln(\omega^2 + a) - \ln(\omega^2 + b) \right\} = \sqrt{a} - \sqrt{b} . \tag{2.69}$$

If we choose $a = U_+(-\bar{\lambda} + \mathrm{e}_s^X(\mathbf{k}))$ and $b = 1$ Eq. (2.68) becomes

$$E^X = \sum_{\mathbf{k},s} \sqrt{U_+(\mathrm{e}_s^X(\mathbf{k}) - \bar{\lambda})}, \tag{2.70}$$

where we have thrown away constant terms since they only change the free energy by an additive constant.

We are now left with the task of computing the fermion free energy. We have a simple intuitive result for the free energy in terms of the Fermi surface. At $T = 0$ the ground state of the fermion sector will be a configuration with all momentum states occupied up to the chemical potential. As such we may simply write down the ground state energy of the fermion sector

$$E^f = \sum_{\mathbf{k},\sigma \atop s,a} \left(\mathrm{e}_{as\sigma}^f(\mathbf{k}) - \mu_a^f \right) \Theta \left(\mu_a^f - \mathrm{e}_{as\sigma}^f(\mathbf{k}) \right) , \tag{2.71}$$

where

$$e^f_{sa\sigma}(\mathbf{k}) = -\frac{t'}{2}\delta_{a1}\left[A_\sigma(\mathbf{k},\phi) + B_\sigma(\mathbf{k},\phi)\right] + \frac{s}{2}\left\{\left[t'(A_\sigma(\mathbf{k},\phi) + B_\sigma(\mathbf{k},\phi))\right]^2\delta_{a1} - 4\left[(t')^2 A_\sigma(\mathbf{k},\phi)B_\sigma(\mathbf{k},\phi)\delta_{a1} - t^2|\Omega^X_{\mathbf{k}}|^2\right]\right\}^{1/2}, \quad (2.72)$$

with

$$\begin{aligned}
\Omega^X_{\mathbf{k}} &= \chi^X_1 + \chi^X_2\left[e^{-i\mathbf{k}\cdot\mathbf{a}_2} + e^{i\mathbf{k}\cdot\mathbf{a}_1}\right] \\
A_\sigma(\mathbf{k},\phi) &= 2\chi^{X'}_1\cos(\mathbf{k}\cdot[\mathbf{a}_1+\mathbf{a}_2] - \sigma\phi) + 2\chi^{X'}_2[\cos(\mathbf{k}\cdot\mathbf{a}_2 + \sigma\phi) + \cos(\mathbf{k}\cdot\mathbf{a}_1 + \sigma\phi)] \\
B_\sigma(\mathbf{k},\phi) &= 2\chi^{X'}_1\cos(\mathbf{k}\cdot[\mathbf{a}_1+\mathbf{a}_2] + \sigma\phi) + 2\chi^{X'}_2[\cos(\mathbf{k}\cdot\mathbf{a}_2 - \sigma\phi) + \cos(\mathbf{k}\cdot\mathbf{a}_1 - \sigma\phi)].
\end{aligned} \quad (2.73)$$

With the above results we can now write the ground state energy density as

$$e = \frac{1}{nN}\left(E^0 + E^f + E^X\right), \quad (2.74)$$

where n is the number of sites per unit cell, 2 for the honeycomb lattice, and N is the total number of unit cells.

Now that we have the ground state energy we may find the zero temperature phase diagram by minimizing the energy with respect to all mean-field order parameters and Lagrange multipliers at each value of the microscopic parameters t, t', and U.

2.5 Self-consistent Equations

In the above analysis we have introduced mean-field order parameters that take the form of valence bonds on the honeycomb lattice. Our saddle point approximation was then achieved by letting these fields, along with the various chemical potentials, take on their saddle point values. In order to determine these values we solve a set of self-consistent equations which are obtained by minimizing the free energy density, Eq. (2.74).

The free energy density is given by

$$\begin{aligned} e &= \frac{1}{2N}\left(E^0 + E^f + E^X\right) \\ &= t\left[\chi_1^f \chi_1^X + 2\chi_2^f \chi_2^X\right] + t'\left[2\chi_1^{f'}\chi_1^{X'} + 4\chi_2^{f'}\chi_2^{X'}\right] + \left[\mu_1 + \mu_2 + \bar{\lambda} + \bar{h}\right] \\ &\quad + \frac{1}{2N}\left[\sum_{\substack{\mathbf{k},\sigma \\ s,a}} \left(\mathrm{e}^f_{as\sigma}(\mathbf{k}) - \mu_a^f\right)\Theta\left(\mu_a^f - \mathrm{e}^f_{as\sigma}(\mathbf{k})\right) + \sum_{\mathbf{k},s}\sqrt{U_+(\mathrm{e}_s^X(\mathbf{k}) - \bar{\lambda})}\right] . \end{aligned} \tag{2.75}$$

If we vary this equation with respect to the field $\bar{h}$ we arrive at the conclusion that $\bar{h} = 0$. Since we are interested in the zero temperature behavior we will compute the chemical potentials for the fermions, μ_1 and μ_2 so that the fermions are at half filling in each layer. The field $\bar{\lambda}$ is determined by the equation

$$\frac{\partial e}{\partial \bar{\lambda}} = 0 = 1 - \frac{U_+}{4N}\sum_{\mathbf{k},s}\frac{1}{\sqrt{U_+(\mathrm{e}_s^X(\mathbf{k}) - \bar{\lambda})}} . \tag{2.76}$$

By minimizing (2.75) with respect to each order parameter we find the self-consistent equations for the valence bond order parameters to be

$$\frac{\partial e}{\partial \chi_\alpha^f} = 0 = \alpha t \chi_\alpha^X + \frac{U_+}{4N}\sum_{\mathbf{k},s}\frac{1}{\sqrt{U_+(\mathrm{e}_s^X(\mathbf{k}) - \bar{\lambda})}}\frac{\partial \mathrm{e}_s^X(\mathbf{k})}{\partial \chi_\alpha^f} \tag{2.77}$$

$$\frac{\partial e}{\partial \chi_\alpha^X} = 0 = \alpha t \chi_\alpha^f + \frac{1}{2N}\sum_{\substack{\mathbf{k},s \\ a,\sigma}}\Theta\left(\mu_a^f - \mathrm{e}^f_{as\sigma}(\mathbf{k})\right)\frac{\partial \mathrm{e}^f_{as\sigma}(\mathbf{k})}{\partial \chi_\alpha^X} \tag{2.78}$$

$$\frac{\partial e}{\partial \chi_\alpha^{f'}} = 0 = 2\alpha t' \chi_\alpha^{X'} + \frac{U_+}{4N}\sum_{\mathbf{k},s}\frac{1}{\sqrt{U_+(\mathrm{e}_s^X(\mathbf{k}) - \bar{\lambda})}}\frac{\partial \mathrm{e}_s^X(\mathbf{k})}{\partial \chi_\alpha^{f'}} \tag{2.79}$$

$$\frac{\partial e}{\partial \chi_\alpha^{X'}} = 0 = 2\alpha t' \chi_\alpha^{f'} + \frac{1}{2N}\sum_{\substack{\mathbf{k},s \\ a,\sigma}}\Theta\left(\mu_a^f - \mathrm{e}^f_{as\sigma}(\mathbf{k})\right)\frac{\partial \mathrm{e}^f_{as\sigma}(\mathbf{k})}{\partial \chi_\alpha^{X'}} , \tag{2.80}$$

where the index $\alpha = 1, 2$ indicates the order parameters we have defined in Fig. 2.3.

Chapter 3

Results and Low Energy Behavior for $U' = 2U$

Now that we have the self-consistent equations (2.76) through (2.80) we may solve them for given values of t, t', and U_+. We solve these equations for all parameters using Newtons method algorithm supplied by the *Numerical Recipes in C* handbook [32].

We solve the self-consistent equations for given t, t', and U_+ within *both* ansatze. The ground state of the system for given coupling constants is then be chosen by identifying the ansatz with the lowest free energy. Choosing the ground state configuration this way allows us to plot the phase diagram of the system quite easily.

3.1 Results

After solving the self-consistent equations we obtain a phase diagram, Fig. 3.2, in the space of t'/t and U/t. We see that there are three distinct regions. We will now describe each of these regions and identify the low energy excitations.

In the small U/t region the system approaches a noninteracting model with no coupling between the layers. In this region the valence bond order parameters for both the chargeons and spinons are in their uniform phase and nonzero as is shown in Fig. 3.1. The Bose condensation amplitude, Z, of the chargeons is nonzero implying that the $U(1)$ gauge field is screened so the low energy excitations of this region are electrons. Here the first layer forms a conventional quantum spin Hall phase with gapless edge modes and a gapped bulk, while the second layer is in a semi-metallic phase with gapless Dirac

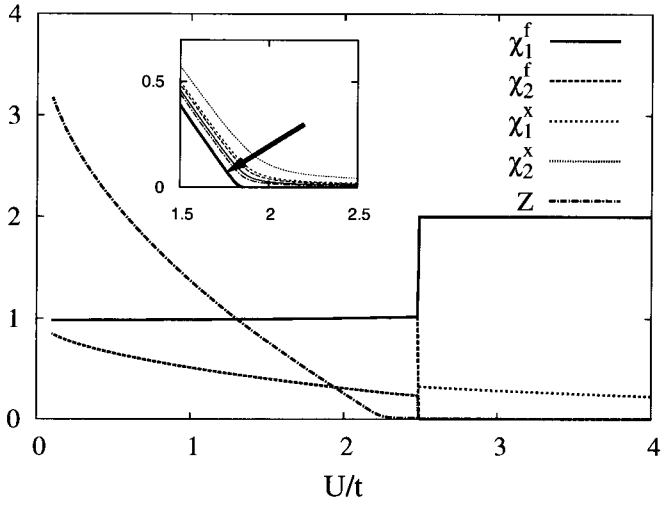

Figure 3.1: Ground state order parameter configurations for $t'/t = 0.5$ on a 40x40 lattice. The first order phase transition between the dimer and uniform configurations can clearly be seen. The inset shows the results of finite size scaling applied to the second order Bose condensation line using lattice sizes in the range of $L = 6$ to $L = 50$ and $t'/t = 0.2$. As we increase the lattice size we see the second order line getting pushed farther back from the first order line. The bold line in the inset is the Bose condensation amplitude in the limit that $L \to \infty$. The first order line is insensitive to the finite size scaling which shows that the window gets larger in the thermodynamic limit and suggest that the fractionalized phase is stable.

fermions.

When $U >> t, t'$ the Coulomb interactions are the dominant term in the Hamiltonian and the low energy states are all possible configurations which satisfy $\sum_a n_{ia} = 2$. We find that the valence bond order parameters for both the chargeons and spinons are in the dimer phase with the dimerized order parameters nonzero while all other valence bond order parameters are zero and $Z = 0$, as shown in Fig. 3.1. Hence both the spinons and chargeons are gapped out. Both layers of the lattice form a symmetry broken insulating phase. Since we have no gapless modes this region has no low energy excitations.

The intermediate region we can see a window has opened up in Fig. 3.1 between the two conventional phases. In this window the valence bond parameters for both chargeons and spinons are in their uniform phase but the chargeons are not condensed. Since the chargeons are not condensed this phase is an insulating phase. In the first layer the spinons are gapped in the bulk due to the spin dependent next nearest neighbour hopping term which arises due to spin-orbit coupling. Ignoring fluctuations of the order parameters we find that the spinon spectrum is essentially the same as the electron spectrum

in the Kane and Mele model [1]. The nontrivial topological structure of this spectrum guarantees that there are gapless edge modes in the first layer. Thus the first layer forms the *fractionalized* quantum spin Hall effect where the edge modes are carried by spinons alone. In the second layer the spinons form an algebraic spin liquid [21] whose low energy excitations are 4 two-component Dirac fermions. It is important to note here that the gapless $U(1)$ gauge field survives because the chargeons do not condense and screen it out.

Upon finite size scaling we find that the second order line recedes from the first order line until it reaches its thermodynamic limit. In the inset of Fig. 3.1 we show the results of finite size scaling of the Bose condensation line for $t'/t = 0.5$. The finite size scaling is done by fitting the Bose condensation to a power series in inverse lattice size

$$Z = \sum_n a_n \left(\frac{1}{L}\right)^n . \tag{3.1}$$

For each value of U/t and t'/t we obtain the coefficients $\{a_n\}$ through a least squares fit and take the limit $(L \to \infty)$. The Bose condensation amplitude in the thermodynamic limit is given by the a_0 coefficient. As we crank up the system size the kink in the second order line becomes more pronounced like a true second order phase transition. The first order line is found to be insensitive to finite size scaling.

3.2 Low Energy Theory of the Fractionalized Phase

The low energy behavior of the fractionalized phase, intermediate window of Fig. 3.2, is determined by the band structure of the spinons and the symmetry of the microscopic model. As discussed above this phase is characterized by a gapless $2+1$ D spinon in the second layer and a gapless $1+1$ D spinon that lives on the edge of the first layer. These two spinons are also coupled to the $U(1)$ gauge field which describes the phase fluctuations of the hopping order parameters. With these three ingredients the low energy theory of

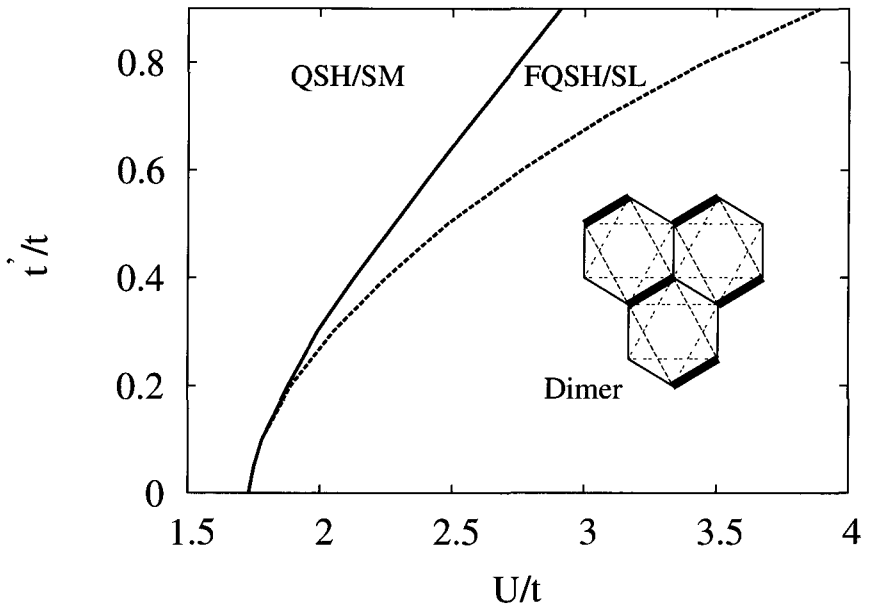

Figure 3.2: Phase diagram in the space of t'/t and U/t in a 40×40 lattice with $U_- = 0$. The weakly interacting phase (small U) has $Z \neq 0$ and the first layer forms the conventional quantum spin Hall (QSH) phase while the second layer is in the semi-metal (SM) phase with gapless Dirac nodes. The intermediate region has the fractionalized quantum spin Hall (FQSH) phase with $Z = 0$ where chargeless spinons form the QSH phase in the first layer and the gapless spin liquid (SL) phase in the second layer. In both QSH/SM and FQSH/SL phases, the nearest neighbour and next-nearest neighbour hopping order parameters are nonzero and site-independent. The large U region is a dimerized phase where the hopping order parameters along the bold lines have the maximum amplitude and all other bonds have zero amplitude. The solid line represents the second order transition and the dotted line, the first order transition.

the fractionalized phase is

$$S_{\text{FQSH}} = \int d^2x d\tau \sum_{n,\sigma} \bar{\psi}_{n\sigma}(i\gamma^\mu D_\mu)\psi_{n\sigma} + \int dx d\tau\ \bar{\eta}(i\gamma^a D_a)\eta + \frac{1}{g^2}\int d^2x d\tau f_{\mu\nu}f^{\mu\nu}\ , \tag{3.2}$$

where $\psi_{n\sigma}$ is a $2+1$ D massless Dirac fermion in the second layer, σ labels the spin, $n = 1, 2$ labels the nodal points of the lattice. $D_\mu = \partial_\mu - ia_\mu$ is the covariant derivative, a_μ is the internal gauge field, and $f_{\mu\nu}$ is the field strength tensor. η is the $1+1$ D massless Dirac fermion on the edge of the first layer, and $a = 0, 1$. We have defined γ^μ and γ^a to be the $2+1$ D and $1+1$ D Dirac matrices, respectively. The constant g is the coupling constant of the $U(1)$ gauge field. We will refer back to this low energy theory when we

discuss the stability of the fractionalized phase.

Chapter 4

Physical Properties of the Fractionalized Quantum Spin Hall Effect

Since the fractional quantum spin Hall state we have studied has gapless edge modes that do not carry charge the transport properties will be very different from the conventional quantum spin Hall state.

Since the spinons carry entropy there will be metallic longitudinal thermal conductivity at the edges of the sample. However, since the low energy theory does not contain any charge degrees of freedom there will be a notable absence of longitudinal charge conductivity along the edges of the sample. The absence of this electromagnetic response of the edges is a signature of spin-charge separation in the system and may be used as a probe to identify the fractionalized phase.

The absence of electromagnetic response also gives rise to the most stark difference between the fractionalized state and the conventional quantum spin Hall state. In the conventional state with conservation of S_z there can be an induced spin transport between the edges of the system. Due to Laughlin's argument [33], if we put the conventional system on a cylinder so that it has two edges and thread a unit magnetic flux quantum through the halo of the cylinder a spin down will be transferred from one edge to the other while a up spin in transferred in the opposite direction, Fig. 4.1(a). Since these electrons are transferred in different directions time-reversal symmetry is preserved.[1] This results

[1]This transfer of spin between the edges and the use of Laughlin's argument requires the conservation of S_z. When S_z is conserved the edge states are analogous to two copies of quantum Hall edge states

in an overall spin transfer of $S = 1$ between the edges. However, due to spin-charge separation in the fractionalized case this effect will be absent since the spinons will not couple to the magnetic field, Fig. 4.1(b). The absence of induced spin transport between the edges could serve as a smoking gun in identifying the fractionalized phase. Since the edge states of the fractionalized quantum spin Hall effect are insensitive to electromagnetic fluctuations one may be able to come up with applications where they may be used.

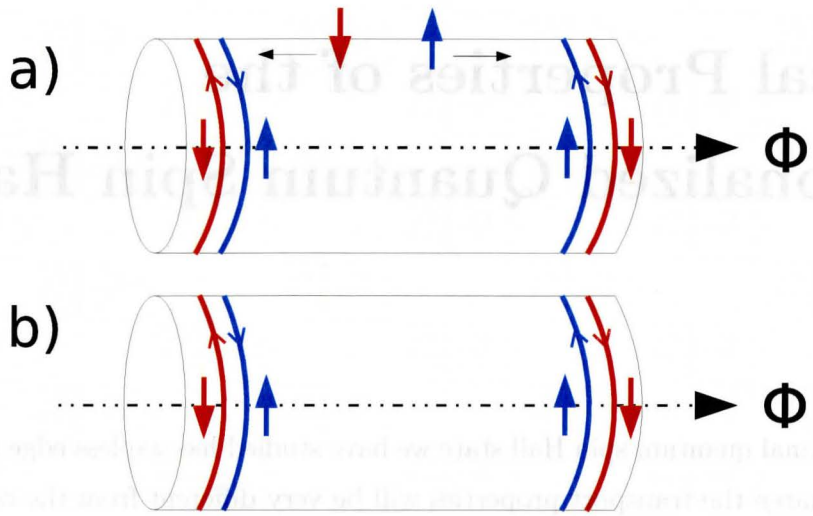

Figure 4.1: Physical properties of the edge states of both the conventional quantum spin Hall effect, Fig.(a), and the fractionalized quantum spin Hall effect, Fig.(b). Upon threading of quantized magnetic flux through the conventional system spin $S = 1$ is transferred between the edges, while in the fractionalized case this does not happen due to the gapped chargeon.

which do not mix. Since they do not mix we can apply Laughlin's argument without any ambiguities.

Chapter 5

Stability of the Edge States

In this chapter we will examine the stability of the fractionalized quantum spin Hall state in the presence of many-body interactions.

The stability of the edge states in the conventional quantum spin Hall states has been well studied [10, 11]. Without the inclusion of interactions the edge states of the quantum spin Hall state are stable due to the presence of a $\mathbb{Z}_2$ topological invariant [3]. This invariant separates systems with even and odd numbers of Kramers pairs into two distinct classes. When the edge states contain an even number of Kramers pairs the system is adiabatically connected to a conventional insulator while a system with an odd number of Kramers pairs cannot be smoothly deformed into a conventional insulator so it belongs to a different universality class. This nontrivial topological order is protected by the time-reversal symmetry of the band structure.

When interactions are added, forward and umklapp scatterings are important in the formation of a gap in the edge states. These two terms are given by

$$H_{\text{fw}} = g \int dx\, \psi^\dagger_{\text{R}\uparrow}\psi_{\text{R}\uparrow}\psi^\dagger_{\text{L}\downarrow}\psi_{\text{L}\downarrow}, \tag{5.1}$$

and

$$H_{\text{um}} = g_u \int dx\, \mathrm{e}^{-4ik_f x}\psi^\dagger_{\text{R}\uparrow}(x)\psi^\dagger_{\text{R}\uparrow}(x+a)\psi_{\text{L}\downarrow}(x+a)\psi_{\text{L}\downarrow}(x) + \text{h.c.}\,, \tag{5.2}$$

respectively. Here $\psi_{R\sigma}(\psi_{L\sigma})$ indicates the edge modes moving in the right(left) direction with spin $\sigma = \uparrow, \downarrow$, while k_f is the Fermi wave vector. The forward scattering term does not open up a gap by itself since it does not mix left and right movers. Since forward scattering only scatters right(left) movers into right(left) movers it can only renormalize the velocity with which the left and right movers travel [10]. However, if one considers

both forward and umklapp scattering at the same time it can be shown that a gap can open up for the edge states if the strength of the forward scattering term is strong enough since the scaling dimension of the umklapp term is a function of the strength of forward scattering [10], g. However, so long as g remains small the umklapp term will remain irrelevant and the gap will vanish in the low energy limit.

In the fractionalized model the situation is a little less clear due to the presence of a gapless spinon in the second layer. Since we allow the first and second layers to interact with via a short range Coulomb term long range correlations of the edge modes in the first layer may occur which can open up a gap in these modes.

Consider a semi-finite strip with an edge along the x_1 direction. Given the low energy theory, Eq. (3.2), and ignoring gauge fluctuations, we ask what will happen if we add interactions. Since we ignore tunneling between the two layers, the lowest order interlayer interaction that couples the two layers is a two body term of the form

$$V \int dx_1 d\tau \; \bar{\psi}(\tau, x_1, x_2 = 0)\psi(\tau, x_1, x_2 = 0)\bar{\eta}(\tau, x_1)\eta(\tau, x_1) \; . \tag{5.3}$$

Since the edge states in the first layer can only interact locally with the bulk states in the second layer the integration measure only has one spatial and one temporal component. Under a scale transformation $(\mathbf{x}, \tau) \rightarrow b(\mathbf{x}', \tau')$ the fields transform as $\psi \rightarrow b^{-1}\psi'$ and $\eta \rightarrow b^{-1/2}\eta'$. If we neglect gauge fluctuations and forward scattering of the edge modes the interaction term scales as $V' = b^{-1}V$. Thus interactions of the form (5.3) are irrelevant at low energies and the edge modes should be stable.

However, if we were to include forward scattering terms for the edge modes of the form

$$u \int dx d\tau \, \bar{\eta}\bar{\eta}\eta\eta \, , \tag{5.4}$$

and gauge fluctuations the edge modes in the first layer will be described by a Luttinger liquid with a nontrivial Luttinger parameter $K \neq 1$ [10], while the spinons in the second layer are described by an algebraic spin liquid. As a result the scaling dimension of V will be modified due to loop corrections and become on the order of $[V] = -1 + O(1/N) + O(K-1)$; Here N is the number of matter fields. Since $N = 4$ in our model the interlayer coupling may remain irrelevant and the edge modes will be stable so long as the forward scattering is sufficiently weak.

Apart from the interlayer interaction, one has also has to worry about the affect of

gauge fluctuations on the stability of the edge modes. In the presence of fluctuating massless $U(1)$ gauge fields the stability of the non-trivial topological order associated with the spinon bands is uncertain. If these fluctuations were to destroy this topological order the edge modes would acquire a gap. To determine the fate of the edge modes one can integrate out the bulk spinons in the low energy theory Eqn. 3.2 to obtain a $1+1$ D effective action for the edge states coupled to the $U(1)$ gauge field. If we do this we would obtain a $1+1$ D quantum electrodynamics (QED) with a non-local action for the gauge field; the specific form of the non-local action is not important. In $1+1$ D QED quantum fluctuations of the gapless fermions open up a gap for the gauge field [34]. Since the gauge field will have a gap its fluctuations will be suppressed at the edge; hence the edge modes will not be greatly affected by fluctuations of the gauge field.

Chapter 6

Away from $U' = 2U$

Previously we assumed a special value for the interlayer interaction energy, $U' = 2U$. As we have previously stated, when we choose this value our problem is reduced to one boson. This reduction to a one boson problem allows us to carry out the above analysis that led to the free energy without any technical problems.

From the discussion in section 2.3 we know, through the Higgs mechanism, that in a finite region around $U' = 2U$ the one boson model remains valid. However, we cannot say anything concretely when we are far away from $U' = 2U$. Since the phase diagram we have computed, Fig. 3.2, has a fractionalized phase one might expect that away from the special value another interesting phase might emerge. Studying this possibility is our chief concern in this chapter.

In addition to being idealized, choosing this value is also somewhat unphysical since it assumes that the electrons couple with more strength between the layers than they do within the layers. To gain more insight into an actual physical system we need to study our model away from the special value of U'.

Since the full theory which includes both bosons and fermions is difficult to analyze we will consider a toy model which has only bosonic degrees of freedom.

6.1 $\mathbb{Z}_2$ Gauge Theory of the Boson Sector

We will simplify this problem by ignoring the fermions and the $U(1)$ gauge field, which reduces our previous Hamiltonian to a toy model for the bosons which is two copies of the Bose-Hubbard model, one for each layer, with interactions coupling the two species

of bosons. The Hamiltonian is

$$H = U \sum_{i,a} n_{ia}^2 + U' \sum_{i} n_{i1} n_{i2} - \sum_{(i,j),a} t \left[\mathrm{e}^{i(\theta_{ia} - \theta_{ja})} + \mathrm{h.c.} \right], \tag{6.1}$$

where U and U' are the intralayer and interlayer Coulomb terms. We take the hopping integral to be uniform on both layers. Note also that we have shifted the number operators from $(n_{ia} - 1)^2$ to simply n_{ia}^2. For the moment we will forgo any discussion on lattice structure.

When $U, U' > t$, the interaction energy becomes more important than the kinetic energy. Here we will make a change of basis to one in which the interaction terms become diagonal. We introduce symmetric and anti-symmetric variables, $n_{i\pm} = n_{i1} \pm n_{i2}$ and $\theta_i^{\pm} = 1/2\,(\theta_{i1} \pm \theta_{i2})$. Note that the new operators are canonically conjugate to each other, $[n_{i\pm}, \theta_i^{\pm}] = i$. With this change of variables the Hamiltonian becomes

$$H = \left(\frac{U}{2} + \frac{U'}{4} \right) \sum_{i} n_{i+}^2 + \left(\frac{U}{2} - \frac{U'}{4} \right) \sum_{i} n_{i-}^2 - \sum_{(i,j)} 4t \cos(\theta_i^+ - \theta_j^+) \cos(\theta_i^- - \theta_j^-), \tag{6.2}$$

where the second term may be written as a cosine due to the Hermitian conjugate term in the hopping sector. We will henceforth let the index α run over $+$ and $-$, and write Hamiltonian (6.2) as

$$H = \sum_{i,\alpha} U_\alpha n_{i\alpha}^2 - \sum_{(i,j)} 4t \cos(\theta_i^+ - \theta_j^+) \cos(\theta_i^- - \theta_j^-), \tag{6.3}$$

where $U_\pm = U/2 \pm U'/4$.

Here we note that we have enlarged the Hilbert space. Only half of the new space of states represents physical states of the system, Fig 6.1. We can see this by noting that for, say, $n_+ = 1$ and $n_- = 0$ we have $n_1 = 1/2$ which is clearly unphysical. In order to project out the unphysical states we impose the constraint that the sum $n_+ + n_-$ is an even number.

In order to calculate the partition function with a constraint we need to define a constraint operator. Such an operator will be zero when acting on an unphysical state and the identity when acting on a physical state. We may write a one site projector for our constraint as

$$\mathcal{P}_{o.s.} = \frac{1}{2} \left(1 + (-1)^{n_+ + n_-} \right). \tag{6.4}$$

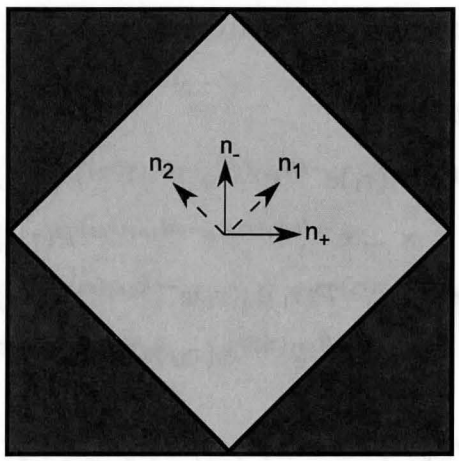

Figure 6.1: The configuration space in the bonding/anti-bonding basis (dark grey) is larger than that of the conventional basis (light gray) by a factor of two. The origin of both bases is given by the coordinate axes in the centre of the squares.

The projector for the full lattice is given simply by taking the product over all lattice sites

$$\mathcal{P} = \prod_i \frac{1}{2}\left(1 + (-1)^{n_{i+}+n_{i-}}\right). \tag{6.5}$$

The projector, (6.5), can be simplified through the inclusion of a $\mathbb{Z}_2$ gauge field $\eta_i = 0, 1$. We may then write

$$\mathcal{P} = \prod_i \frac{1}{2} \sum_{\eta_i=0,1} \mathrm{e}^{i\pi\eta_i(n_{i+}+n_{i-})}. \tag{6.6}$$

The partition function is then calculated as

$$\mathcal{Z} = \mathrm{Tr}\left[\mathrm{e}^{-\beta H}\mathcal{P}\right], \tag{6.7}$$

where the trace now involves a sum over the gauge fields $\{\eta\}$ on each site as well as the sums over $\{n\}$ and $\{\theta\}$. To compute this we use the standard trick of splitting up the exponential in a time-ordered product of operators. We have

$$\mathcal{Z} \approx \mathrm{Tr}\left[\left(\mathrm{e}^{-\epsilon H}\mathcal{P}\right)^M\right] \approx \mathrm{Tr}\left[\left(\mathrm{e}^{-\epsilon H_{\{\theta\}}}\mathrm{e}^{-\epsilon H_{\{n\}}}\mathcal{P}\right)^M\right],$$

where $H_{\{n\}} = +\sum_{i,\alpha} U_\alpha n_{i\alpha}^2$ and $H_{\{\theta\}} = -\sum_{(i,j)} 4t\cos(\theta_i^+ - \theta_j^+)\cos(\theta_i^- - \theta_j^-)$. To compute the partition function here we will again use the basis of coherent states for the phase operators θ_i^α, appendix D.

We are now in shape to compute the effective action.

$$\begin{aligned}
\mathcal{Z} &\approx \mathrm{Tr}\left[\left(\mathrm{e}^{-\epsilon H_{\{\theta\}}}\mathrm{e}^{-\epsilon H_{\{n\}}}\mathcal{P}\right)^{M}\right] \\
&= \mathrm{Tr}\left[\mathrm{e}^{-\epsilon H_{\{\theta\}}(\tau_1)}\mathrm{e}^{-\epsilon H_{\{n\}}(\tau_1)}\mathcal{P}(\tau_1)\mathrm{e}^{-\epsilon H_{\{\theta\}}(\tau_2)}\mathrm{e}^{-\epsilon H_{\{n\}}(\tau_2)}\mathcal{P}(\tau_2)\ \ldots\right. \\
&\qquad\qquad \left.\times\ \ldots\ \mathrm{e}^{-\epsilon H_{\{\theta\}}(\tau_M)}\mathrm{e}^{-\epsilon H_{\{n\}}(\tau_M)}\mathcal{P}(\tau_M)\right] \\
&= \mathrm{Tr}\left[\mathrm{e}^{-\epsilon H_{\{\theta\}}(\tau_1)}\mathbb{I}_\theta(\tau_1)\mathrm{e}^{-\epsilon H_{\{n\}}(\tau_1)}\mathcal{P}(\tau_1)\mathbb{I}_n(\tau_1)\mathrm{e}^{-\epsilon H_{\{\theta\}}(\tau_2)}\mathbb{I}_\theta(\tau_2)\mathrm{e}^{-\epsilon H_{\{n\}}(\tau_2)}\mathcal{P}(\tau_2)\mathbb{I}_n(\tau_1)\right. \\
&\qquad\qquad \left.\ldots\ \mathrm{e}^{-\epsilon H_{\{\theta\}}(\tau_M)}\mathbb{I}_\theta(\tau_M)\mathrm{e}^{-\epsilon H_{\{n\}}(\tau_M)}\mathcal{P}(\tau_M)\mathbb{I}_n(\tau_M)\right], \qquad (6.8)
\end{aligned}$$

where the identities are given by

$$\mathbb{I}_n(\tau_\mu) = \prod_{i,\alpha}\sum_{n_{i\alpha}} |n_{i\alpha}(\tau_\mu)\rangle\langle n_{i\alpha}(\tau_\mu)| \quad \text{and} \quad \mathbb{I}_\theta(\tau_\mu) = \int \prod_{i,\alpha} \frac{d\theta_i^\alpha(\tau_\mu)}{2\pi} |\theta_i^\alpha(\tau_\mu)\rangle\langle\theta_i^\alpha(\tau_\mu)|. \quad (6.9)$$

Evaluating all of the inner products we arrive at the effective action

$$\begin{aligned}
S &= -i\sum_{\mu=0}^{M}\sum_{i,\alpha} n_{i\alpha}(\tau_\mu)\left[\theta_i^\alpha(\tau_\mu) - \theta_i^\alpha(\tau_{\mu+1}) + \pi\eta_i(\tau_\mu)\right] + \sum_{\mu=0}^{M}\epsilon H(\tau_\mu) \\
&= \sum_{\mu=0}^{M}\sum_{i,\alpha}\left\{\epsilon U_\alpha n_{i\alpha}^2(\tau_\mu) - i n_{i\alpha}(\tau_\mu)\left[\theta_i^\alpha(\tau_\mu) - \theta_i^\alpha(\tau_{\mu+1}) + \pi\eta_i(\tau_\mu)\right]\right\} \\
&\quad -4\epsilon t\sum_{\mu=0}^{M}\sum_{(i,j)}\cos(\theta_i^+(\tau_\mu) - \theta_j^+(\tau_\mu))\cos(\theta_i^-(\tau_\mu) - \theta_j^-(\tau_\mu)), \qquad (6.10)
\end{aligned}$$

where we have used periodic boundary conditions $\theta_i^\alpha(\tau_M) = \theta_i^\alpha(\tau_0)$ and $n_{i\alpha}(\tau_M) = n_{i\alpha}(\tau_0)$. The partition function is then given by

$$\mathcal{Z} = \left(\prod_{\mu=0}^{M}\prod_{i,\alpha}\int_0^{2\pi}\frac{d\theta_i^\alpha(\tau_\mu)}{2\pi}\right)\left(\prod_{\mu=0}^{M}\prod_{i,\alpha}\sum_{n_{i\alpha}(\tau_\mu)=-\infty}^{+\infty}\right)\mathrm{e}^{-S}\,. \qquad (6.11)$$

We can perform the sum over the number operator eigenvalues in the same manner we have done previously. We define new variables $\tilde{n}_{i\alpha} = \epsilon n_{i\alpha}$. With this change we can convert the sum to an integral in the limit the ϵ is small. Since the action is local in the variables $\tilde{n}_{i\alpha}$ we may then perform the Gaussian integrals to get

$$\mathcal{Z} = \left(\prod_{\mu=0}^{M}\prod_{i,\alpha}\int_0^{2\pi}\frac{d\theta_i^\alpha(\tau_\mu)}{2\pi}\right)\left(\prod_{\mu=0}^{M}\prod_{i,\alpha}\sqrt{\frac{\pi}{\epsilon^3 U_\alpha}}\right)\mathrm{e}^{-S_{eff}}, \qquad (6.12)$$

where the effective action is

$$\begin{aligned} S_{eff} &= \epsilon \sum_{\mu=0}^{M} \sum_{i,\alpha} \frac{1}{4U_\alpha} \left[\Delta_\epsilon \theta_i^\alpha(\tau_\mu) + \frac{\pi}{\epsilon} \eta_i(\tau_\mu) \right]^2 \\ &\quad -4\epsilon t \sum_{\mu=0}^{M} \sum_{(i,j)} \cos(\theta_i^+(\tau_\mu) - \theta_j^+(\tau_\mu)) \cos(\theta_i^-(\tau_\mu) - \theta_j^-(\tau_\mu)), \end{aligned} \tag{6.13}$$

and we have introduced the lattice time derivative

$$\Delta_\epsilon \theta_i^\alpha(\tau_\mu) = \frac{\theta_i^\alpha(\tau_\mu) - \theta_i^\alpha(\tau_{\mu-1})}{\epsilon}. \tag{6.14}$$

This action is invariant under the $\mathbb{Z}_2$ gauge transformations

$$\theta_i^\alpha(\tau_\mu) \rightarrow \theta_i^{\alpha'}(\tau_\mu) + \pi\nu_i(\tau_\mu) \qquad \eta_i(\tau_\mu) \rightarrow \eta_i'(\tau_\mu) - \nu_i(\tau_\mu) + \nu_i(\tau_{\mu-1}), \tag{6.15}$$

where $\eta_i(\tau_\mu) = 0, 1$ is the time component of the $\mathbb{Z}_2$ gauge field.

To reveal the full gauge structure of the model we decouple the quartic terms with a Hubbard-Stratonovich transformation. There is one caveat however. Since the different flavours of boson fields ($\pm$) are not treated on equal footing we cannot simply use one Hubbard-Stratonovich field for both. We must allow the fields to have different weights. Thus we write

$$\begin{aligned} &e^{4\epsilon t \sum_{\mu=0}^{M} \sum_{(i,j)} \cos(\theta_i^+(\tau_\mu) - \theta_j^+(\tau_\mu)) \cos(\theta_i^-(\tau_\mu) - \theta_j^-(\tau_\mu))} \\ &\qquad = \prod_{\mu,(i,j)} e^{4\epsilon t \cos(\theta_i^+(\tau_\mu) - \theta_j^+(\tau_\mu)) \cos(\theta_i^-(\tau_\mu) - \theta_j^-(\tau_\mu))}. \end{aligned} \tag{6.16}$$

To minimize the equations let $A_{ij} = \cos(\theta_i^+(\tau_\mu) - \theta_j^+(\tau_\mu))$ and $B_{ij} = \cos(\theta_i^-(\tau_\mu) - \theta_j^-(\tau_\mu))$, then

$$\begin{aligned} &\prod_{\mu,(i,j)} e^{4\epsilon t \cos(\theta_i^+(\tau_\mu) - \theta_j^+(\tau_\mu)) \cos(\theta_i^-(\tau_\mu) - \theta_j^-(\tau_\mu))} \\ &\qquad = \prod_{\mu,(i,j)} e^{4\epsilon t\, A_{ij} B_{ij}} = \prod_{\mu,(i,j)} e^{2\epsilon t (A_{ij} + B_{ij})^2} e^{-2\epsilon t A_{ij}^2} e^{-2\epsilon t B_{ij}^2}. \end{aligned} \tag{6.17}$$

We may now use the Gaussian integral identities

$$e^{2\epsilon t \Delta_{ij}^2} = \sqrt{\frac{\epsilon t}{2\pi}} \int_{-\infty}^{\infty} d\xi_{ij} e^{-\frac{\epsilon t}{2}\xi_{ij}^2 + 2\epsilon t \Delta_{ij} \xi_{ij}}, \tag{6.18}$$

and

$$e^{-2\epsilon t\Delta_{ij}^2} = \sqrt{\frac{\epsilon t}{2\pi}} \int_{-\infty}^{\infty} d\xi_{ij} e^{-\frac{\epsilon t}{2}\xi_{ij}^2 + i2\epsilon t\Delta_{ij}\xi_{ij}} \tag{6.19}$$

for real fields ξ_{ij}, to write

$$\begin{aligned}\prod_{\mu,(i,j)} e^{2\epsilon t(A_{ij}+B_{ij})^2} e^{-2\epsilon t A_{ij}^2} e^{-2\epsilon t B_{ij}^2} &= \prod_{\mu,(i,j)} \left(\prod_{a=1}^{3} \sqrt{\frac{\epsilon t}{2\pi}} \int_{-\infty}^{\infty} d\xi_{ij}^a \right) \\ &\times e^{-\frac{\epsilon t}{2}\sum_{a=1}^{3}(\xi_{ij}^a)^2 + 2\epsilon t(\xi_{ij}^1 + i\xi_{ij}^2)A_{ij} + 2\epsilon t(\xi_{ij}^1 + i\xi_{ij}^3)B_{ij}} .\end{aligned} \tag{6.20}$$

We now have the effective action

$$\begin{aligned} S &= \epsilon \sum_{\mu=0}^{M} \sum_{i,\alpha} \frac{1}{4U_\alpha} \left[\Delta_\epsilon \theta_i^\alpha + \frac{\pi}{\epsilon}\eta_i \right]^2 + \frac{\epsilon t}{2} \sum_{\mu,(i,j)} \sum_{a=1}^{3} (\xi_{ij}^a)^2 \\ &\quad -2\epsilon t \sum_{\mu,(i,j)} \left[(\xi_{ij}^1 + i\xi_{ij}^2)\cos(\theta_i^+ - \theta_j^+) + (\xi_{ij}^1 + i\xi_{ij}^3)\cos(\theta_i^- - \theta_j^-) \right], \end{aligned} \tag{6.21}$$

where we have suppressed all time dependence of the fields.

The above action is not real, however, so we must analytically continue the fields ξ^2 and ξ^3 into the complex plane by $\bar{\xi}^2 = i\xi^2$ and $\bar{\xi}^3 = i\xi^3$. The action takes the form

$$\begin{aligned} S &= \epsilon \sum_{\mu=0}^{M} \sum_{i,\alpha} \frac{1}{4U_\alpha} \left[\Delta_\epsilon \theta_i^\alpha + \frac{\pi}{\epsilon}\eta_i \right]^2 + \frac{\epsilon t}{2} \sum_{\mu,(i,j)} (\xi_{ij}^1)^2 - \frac{\epsilon t}{2} \sum_{\mu,(i,j)} \sum_{a=2}^{3} (\bar{\xi}_{ij}^a)^2 \\ &\quad -2\epsilon t \sum_{\mu,(i,j)} \left[(\xi_{ij}^1 + \bar{\xi}_{ij}^2)\cos(\theta_i^+ - \theta_j^+) + (\xi_{ij}^1 + \bar{\xi}_{ij}^3)\cos(\theta_i^- - \theta_j^-) \right]. \end{aligned} \tag{6.22}$$

Before we proceed to analyze this action we consider another special case, $U' = 0$. In this limit our toy model (6.1) reduces to two copies of the Bose-Hubbard model. These models have been well studied so we know what the physics in this limit should be. The Bose-Hubbard model exhibits two phases, one being a conventional insulating phase, the other being a conventional superfuild phase in which the bosons are condensed. To write down the effective action for this case we simply note that when $U' = 0$ the $\pm$ bosons have the same coupling constants and the action should be symmetric in these two fields. This implies that we need only introduce one, complex, auxiliary field in the Hubbard-

Stratonovich transformation. The action is therefor

$$\begin{aligned} S_{U'=0} &= \frac{\epsilon}{2\tilde{U}} \sum_{i,\mu} \sum_{\alpha} \left[\Delta_\epsilon \theta_i^\alpha + \frac{\pi}{\epsilon} \eta_i \right]^2 + 4t\epsilon \sum_{(i,j)} \sum_{\mu} |\xi_{ij}|^2 \\ &\quad -4t\epsilon \sum_{(i,j)} \sum_{\mu} \left[\xi_{ij} \cos(\theta_i^+ - \theta_j^+) + \xi_{ij}^* \cos(\theta_i^- - \theta_j^-) \right], \end{aligned} \tag{6.23}$$

where we have introduced the modified Coulomb energy $\tilde{U} = U/2$ for later convenience.

In order to determine the dynamics of the $\mathbb{Z}_2$ gauge fields we must integrate out the matter fields. However, this is a difficult task with the two actions above written how they are now. To make our job easier we can rewrite the actions to be sums over a space-*time* lattice instead of just a space lattice. To achieve this we note that we may approximate the temporal gradient term, so long as the time step is small, as

$$\begin{aligned} \frac{\epsilon}{2\tilde{U}} \left[\Delta_\epsilon \theta_i^\alpha + \frac{\pi}{\epsilon} \eta_i \right]^2 &\approx \frac{1}{\epsilon\tilde{U}} \mathbb{I} - \frac{1}{\epsilon\tilde{U}} \cos\left(\theta_i^\alpha(\mu) - \theta_i^\alpha(\mu-1) + \pi\eta_i(\mu) \right) \\ &= \frac{1}{\epsilon\tilde{U}} \mathbb{I} - \frac{1}{\epsilon\tilde{U}} \xi_i(\mu) \cos\left(\theta_i^\alpha(\mu) - \theta_i^\alpha(\mu-1) \right) \end{aligned} \tag{6.24}$$

where in the last line we have used the $\mathbb{Z}_2$ nature of the gauge fields to write a temporal component of the gauge field out front of the cosine. The above manipulations allow us to write down the action on the space time lattice as follows

$$S_{U'=0} = \sum_{i,\mu} \left[\frac{2}{\epsilon\tilde{U}} \mathbb{I} \right] + 4t\epsilon \sum_{(i,j)} \sum_{\mu} \xi_{ij}^2 - \sum_{(I,J)} \sum_{\alpha} \tilde{t}_{IJ} \xi_{IJ} \cos(\theta_I^\alpha - \theta_J^\alpha) \tag{6.25}$$

where (I,J) refers to pairs on the space-time lattice, (i,j) refers to pairs on the spacial lattice only, μ is the time slice, and we have let ξ become real valued in order for the action to be real.[1] We have also defined new dimensionless hopping parameters, $\tilde{t}_{IJ}$ which take on different values for spacial and temporal links. For the spacial links $\tilde{t}_{IJ} = 4t\epsilon$ while for temporal links $\tilde{t}_{IJ} = 1/\tilde{U}\epsilon$.

Before integrating out the matter fields we would like to treat space and time on an equal footing. To do this we require that the hopping parameters on each type of link are equal to each other, namely $1/\tilde{U}\epsilon = 4t\epsilon$. This implies that we must work with a time step of $\epsilon = 1/\left[2\sqrt{t\tilde{U}}\right]$, which gives a new, isotropic, hopping parameter as $t_{iso} = 2\sqrt{t/\tilde{U}}$.

[1] This may actually be done in general since the only change in the analytics would be a different numerical factor in the Jacobian, which is just a multiplicative constant to the partition function and thus it does not affect any physical properties of the system.

This allows us to write the action as

$$S_{U'=0} = 2t_{iso}\sum_{i,\mu}\mathbb{I} + t_{iso}\sum_{(i,j)}\sum_{\mu}\xi_{ij}^2 - t_{iso}\sum_{(I,J)}\sum_{\alpha}\xi_{IJ}\cos(\theta_I^\alpha - \theta_J^\alpha). \tag{6.26}$$

Here $\xi = \pm 1$ is the $\mathbb{Z}_2$ gauge field.

Before proceeding with the general case, $U' \neq 0$, we will integrate out the matter fields in the special case and obtain the effective gauge coupling. Here we will take $t_{iso} << 1$ which will allow us to expand the exponential in the partition function as a Taylor series. When we take this limit we are assuming that the bosons are in their insulating phase since $t_{iso} = 2\sqrt{t/\tilde{U}}$, and $\tilde{U}/t$ is proportional to the dimensionless parameter upon which the phase diagram is based. When $\tilde{U}/t$ is large the Coulomb terms win and the bosons want to be as localized as possible suggesting that they are in the insulating phase.

Up to multiplicative constants the partition function for this action is given by

$$\begin{aligned}\mathcal{Z} &= \sum_{\{\xi\}}\int\prod_I \frac{d\theta_I^+}{2\pi}\frac{d\theta_I^-}{2\pi}\mathrm{e}^{-S_{U'=0}} \\ &= \sum_{\{\xi\}}\int\prod_I \frac{d\theta_I^+}{2\pi}\frac{d\theta_I^-}{2\pi}\mathrm{e}^{-2t_{iso}\sum_{i,\mu}\mathbb{I} - t_{iso}\sum_{(i,j)}\sum_{\mu}\xi_{ij}^2}\prod_{(I,J)}\prod_{\alpha}\sum_n\frac{(t_{iso}\xi_{IJ})^n}{2^n n!} \\ &\qquad\times\left[\mathrm{e}^{i(\theta_I^\alpha-\theta_J^\alpha)} + \mathrm{e}^{-i(\theta_I^\alpha-\theta_J^\alpha)}\right]^n. \end{aligned}\tag{6.27}$$

In order to integrate out the matter fields we now define a directed graph. For each

Figure 6.2: Directed link associated with the exponential $\mathrm{e}^{i(\theta_i^\alpha-\theta_j^\alpha)}$. The line connected to the lattice sites represents the $\mathbb{Z}_2$ gauge field; each line comes with a factor of $t_{iso}\xi_{ij}$.

flavour of boson we associate a directed link, Fig. 6.2, with the factor $\mathrm{e}^{i(\theta_i^\alpha-\theta_j^\alpha)}$. Since the integration of the θ fields is over the range $[0, 2\pi]$ any graph with open ends will not give a contribution to the partition function so we can ignore them all.

The lowest order closed diagram is one which contains two internal lines of the same flavour, Fig. 6.3(a). Now comes time where we must fix a lattice to work with. We will choose a 2+1 dimensional cubic lattice with nearest neighbour hopping only, thus

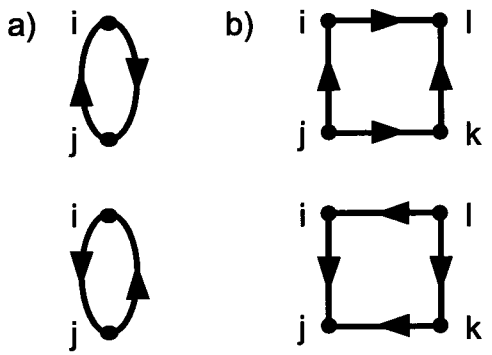

Figure 6.3: The lowest order closed real space diagrams contributing to the partition function. For completeness here we show the Hermitian conjugate of all diagrams.

the pair (i,j) is now understood as a nearest neighbour pairing in the space-time cubic lattice. This choice of lattice now affects the subsequent diagrams that may appear in the expansion. If we were to take, say, a triangular lattice we could have diagrams with three internal lines, which would correspond to cubic terms in the gauge fields. However, no such term is possible on the square lattice with only nearest neighbour coupling. [2] On a cubic lattice with nearest neighbour coupling the next lowest order closed loop is a single plaquette, Fig. 6.3(b).

We may write the partition function for such a plaquette as

$$\begin{aligned}
&\int \frac{d\theta_I^+}{2\pi}\frac{d\theta_I^-}{2\pi}\frac{d\theta_J^+}{2\pi}\frac{d\theta_J^-}{2\pi}\frac{d\theta_K^+}{2\pi}\frac{d\theta_K^-}{2\pi}\frac{d\theta_L^+}{2\pi}\frac{d\theta_L^-}{2\pi}\prod_{\alpha=\pm} \\
&\qquad \times \left[t_{iso}\xi_{IJ}\cos(\theta_I^\alpha - \theta_J^\alpha)\right]\left[t_{iso}\xi_{JK}\cos(\theta_J^\alpha - \theta_K^\alpha)\right] \\
&\qquad \times \left[t_{iso}\xi_{KL}\cos(\theta_K^\alpha - \theta_L^\alpha)\right]\left[t_{iso}\xi_{LI}\cos(\theta_L^\alpha - \theta_I^\alpha)\right] \\
= \; &\frac{t_{iso}^4}{4}\left(\xi_{ij}\xi_{jk}\xi_{kl}\xi_{li}\right). \qquad (6.28)
\end{aligned}$$

Here we have written the boson operators in terms of cosines to minimize the notation.

To obtain the effective action for the gauge field we need to exponentiate this result.

[2] If we also included *next* nearest neighbour terms these diagrams would appear.

However, the details of this calculation may be omitted if we recall the linked cluster theorem. This theorem states that the only diagrams to appear in an effective action are the irreducible ones. We may then use a cumulant expansion to write our effective action as[3]

$$S_{\text{eff}}^{U'=0} = \frac{t_{iso}^4}{4} \sum_{\text{plaq}} \xi_{ij}\xi_{jk}\xi_{kl}\xi_{li}. \tag{6.29}$$

Here we have ignored the constant terms and squared gauge field terms that appear in the partition function since they do not enter into the upcoming discussion. Since the above expansion assumes that the effective hopping parameter is small the effective action (6.29) is only valid in the insulating phase of the Bose-Hubbard phase diagram.

Equation (6.29) is just the action of a $\mathbb{Z}_2$ lattice gauge theory with a Maxwell term [35], represented by the plaquette product. With this effective action we obtain an effective gauge coupling, g, defined by

$$\frac{1}{g^2} = \frac{t_{iso}^4}{4} \, . \tag{6.30}$$

The phase diagram of the $\mathbb{Z}_2$ gauge theory theory in 2+1 D contains two phases [36], a confining phase and a deconfining phase. The phase transition between these two phases will occur at $\frac{1}{g_c^2}$. In the language of lattice gauge theory the conventional insulating phase corresponds to the confined phase. Since we know that the only possible insulating phase is the conventional insulating phase (the confinement phase), our effective gauge coupling should satisfy $\frac{1}{g^2} = \frac{t_{iso}^4}{4} < \frac{1}{g_c^2}$.

The question now is what will happen once we turn on the interactions between the two bosons. Intuitively we should expect that the effective gauge coupling is altered, but the question is *how* it is altered.

To answer this question we study the general case where $U' \neq 0$. The two flavours have different hopping integrals as

$$S_{U'\neq 0} = -\sum_{(i,j)} \sum_{\alpha} t_{iso}^{\alpha} \xi_{ij} \cos(\theta_i^{\alpha} - \theta_j^{\alpha}), \tag{6.31}$$

where $t_{\text{iso}}^{\alpha} = 2\sqrt{t/U_{\alpha}}$, with $\alpha = \pm$. Here we have ignored the squared terms that appear in the $U' = 0$ case since they do not affect the effective gauge coupling. We could have derived this action in the same way we did equation (6.26) but for our purposes we only need the final result.

[3]The numerical factors in the action come from the cumulant expansion.

After performing a small t_{iso}^{α} expansion we obtain the effective action for the general gauge theory,

$$S_{\text{eff}}^{U'\neq 0} = \frac{(t_{iso}^{+})^4 + (t_{iso}^{-})^4}{8} \sum_{\text{plaq}} \xi_{ij}\xi_{jk}\xi_{kl}\xi_{li} \ . \tag{6.32}$$

So when $U' \neq 0$ the effective gauge coupling is

$$\frac{1}{G^2} = \frac{(t_{iso}^{+})^4 + (t_{iso}^{-})^4}{8} \ . \tag{6.33}$$

We use a capital G here to distinguish between $U' = 0$ and $U' \neq 0$.

Now that we know how the effective gauge coupling changes when $U' \neq 0$ we may determine whether or not a deconfined phase of the gauge field is possible. The deconfined phase of the $\mathbb{Z}_2$ gauge field will occur when the matter content is in its insulating phase but at the same time, the gauge coupling becomes smaller than g_c. If this were to happen we would see a window for the deconfined phase open up in the Bose-Hubbard phase diagram in a similar manner that the fractionalized quantum spin Hall phase appears between the insulator and Higgs phases of the Hubbard model above.

In order for the deconfined phase to be possible we must simultaneously satisfy two conditions: 1) The effective coupling when $U' \neq 0$ must be smaller than the effective coupling when $U' = 0$, $G < g$: and 2) The bosons must not be allowed to condense to prevent screening of the gauge field which will cause a phase transition out of the insulating phase into the superfluid phase which implies that the gauge field is in its Higgs phase. This requires $t_{\text{iso}}^{\alpha} < t_{\text{c}}$.

We know that when $U' = 0$ the Hamiltonian (6.1) reduces to two copies of the Bose-Hubbard model which only has two phases. As we have stated above the pure gauge theory is valid only in the insulating phase which implies that the internal gauge field is in its confining phase. Thus the effective coupling constant g is greater than the critical coupling constant g_c where the confinement/deconfinement phase transition occurs, i.e.

$$\frac{1}{g^2} < \frac{1}{g_c^2}. \tag{6.34}$$

When $U' = 0$ we also know that the effective hopping parameters for the $\pm$ bosons become equal, which means that the two flavours of bosons will condense at the same t_c. This is the maximum value that t^{α} may reach before the bosons condense and the gauge field enters into the Higgs phase. The inverse gauge coupling takes on its maximum value

at this point

$$\frac{1}{g^2} \approx 2t_c^4 < \frac{1}{g_c^2}, \tag{6.35}$$

This last inequality comes from the fact that we know that g^2 is larger than g_c^2 for the confinement/deconfinement phase transition since the decoupled Bose-Hubbard model does not have a deconfined phase.

When $U' > 0$ we can set the maximum value of the hopping parameters for the bosons to condense as $t_c = t^-$ since $t^- \equiv 2\sqrt{t/U_-}$ is by definition larger than t^+ for a given t and U. Since this is the case the inverse effective gauge coupling must satisfy

$$\frac{1}{G^2} \approx t^{-4} + t^{+4} < \frac{1}{g^2} \approx 2t_c^4 < \frac{1}{g_c^2} \tag{6.36}$$

since $t^{-4} + t^{+4}$ can never be as large as $2t_c^4$ without the θ^- boson first condensing. Thus a deconfined phase of the gauge field becomes more unlikely with a nonzero U'.

The conclusion we have arrived at suggests that the phase diagram, Fig. 3.2, should not have any additional deconfinement when U' differs from $2U$. However, this conclusion is simply a qualitative one based on the toy Bose-Hubbard model of this chapter.

Chapter 7

Conclusions

In this work we have studied a simple model which we have shown may realize a fractionalized quantum spin Hall phase. We coin this phase the 'fractionalized' quantum spin Hall phase since the edge states that mark the quantum spin Hall phase exhibit spin-charge separation in our model. These spin-charge separated edge states are made up of gapless spinons which carry only spin but no charge.

The absence of charge degrees of freedom in the edge states gives rise to drastic differences in response properties between the conventional and the fractionalized states. The most notable of these differences is the absence of transverse spin transport as shown in Fig. 4.1. The second signature is the absence of longitudinal metallic conductivity along the edge of the sample even though there is longitudinal thermal conductivity. These two properties may be viewed as evidence of spin-charge separation in the sample.

Within the mean-field approximation we find that the fractionalized state is stable in a parameter regime as shown in Fig. 3.2. We have also argued in chapter 5 that the fractionalized phase may be stable beyond the mean-field approximation

The mean-field theory we have derived in chapter 2 is based on a slave-rotor decomposition of the electron operators with valence bond order parameters in $2+1$ D. In general, a theory such as this can have an emergent compact $U(1)$ gauge field which describes the phase fluctuations of the valence bond order parameters due to the $U(1)$ gauge invariance of the slave-rotor decomposition. Since in $2+1$ D the pure compact $U(1)$ gauge field is always confining [26] we needed to introduce additional gapless modes which would screen the gauge field to stabilize the fractionalized phase which has spinons as low energy excitations. In $3+1$ D however, the pure compact $U(1)$ gauge theory can have a stable deconfined phase without gapless matter fields. Hence we may ask the question

whether or not a fractionalized topological insulator with an emergent $U(1)$ gauge boson may be stable in $3+1$ D. $3+1$ D topological insulators, have been studied for some time now [4, 6]. It would be interesting to study the possibility of a fractionalized quantum spin Hall phase in $3+1$ dimensions in the future.

Appendix A

Energy Spectra

In this appendix we derive the energy dispersions of the bosons and fermions. For the bosons the spectrum is found by diagonalizing a Hamiltonian of the form

$$\begin{aligned} H &= -\sum_{(i,j)} \left(t_{ij} \chi^f_{ij} X^*_i X_j + h.c \right) \\ &= -\sum_{<i,j>} \left(t \chi^f_{ij} X^*_i X_j + h.c \right) - \sum_{<<i,j>>} \left(t' \chi^f_{ij} X^*_i X_j + h.c \right) . \end{aligned} \tag{A.1}$$

It will be easier to evaluate the sums if we break up the site index into a unit cell index and a basis index; set $X_i = X_{I\alpha_I}$ where $\alpha_I = A, B$ is the basis index and I is the unit cell index. We can now write out the sums over nearest and next nearest neighbours explicitly. We have

$$\begin{aligned} H &= -t \sum_{\mathbf{J}|} \Big(\chi^f_{\mathbf{J}B\mathbf{J}A} X^*_{\mathbf{J}B} X_{\mathbf{J}A} + \chi^f_{(\mathbf{J}+\mathbf{a_2})B\mathbf{J}A} X^*_{(\mathbf{J}+\mathbf{a_2})B} X_{\mathbf{J}A} \\ &\qquad + \chi^f_{(\mathbf{J}-\mathbf{a_1})B\mathbf{J}A} X^*_{(\mathbf{J}-a_1)B} X_{\mathbf{J}A} + h.c \Big) \\ &\quad -t' \sum_{\mathbf{J},\alpha} \Big(\chi^f_{(\mathbf{J}+\mathbf{a_1}+\mathbf{a_2})\alpha\mathbf{J}\alpha} X^*_{(\mathbf{J}+\mathbf{a_1}+\mathbf{a_2})\alpha} X_{\mathbf{J}\alpha} + \chi^f_{(\mathbf{J}+\mathbf{a_2})\alpha\mathbf{J}\alpha} X^*_{(\mathbf{J}+\mathbf{a_2})\alpha} X_{\mathbf{J}\alpha} \\ &\qquad + \chi^f_{(\mathbf{J}-\mathbf{a_1})\alpha\mathbf{J}\alpha} X^*_{(\mathbf{J}-\mathbf{a_1})\alpha} X_{\mathbf{J}\alpha} + h.c \Big) . \end{aligned} \tag{A.2}$$

Representing the fields in terms of their Fourier components

$$X_{\mathbf{J}\alpha} = \frac{1}{\sqrt{N}} \sum_{\mathbf{k}} e^{i\mathbf{k}\cdot\mathbf{J}} X_{\mathbf{k}\alpha} \tag{A.3}$$

we have

$$\begin{aligned} H &= -\frac{t}{N}\sum_{\substack{\mathbf{k},\mathbf{k}'\\ \mathbf{J}}}\Big(\chi^f_{\mathbf{J}BJA}\mathrm{e}^{-i\mathbf{J}\cdot(\mathbf{k}-\mathbf{k}')}X^*_{\mathbf{k}B}X_{\mathbf{k}'A}+\chi^f_{(\mathbf{J}+a_2)BJA}\mathrm{e}^{-i\mathbf{J}\cdot(\mathbf{k}-\mathbf{k}')}\mathrm{e}^{-i\mathbf{k}\cdot\mathbf{a}_2}X^*_{\mathbf{k}B}X_{\mathbf{k}'A} \\ &+\chi^f_{(\mathbf{J}-\mathbf{a}_1)BJA}\mathrm{e}^{-i\mathbf{J}\cdot(\mathbf{k}-\mathbf{k}')}\mathrm{e}^{i\mathbf{k}\cdot\mathbf{a}_1}X^*_{\mathbf{k}B}X_{\mathbf{k}'A}+h.c\Big) \\ &-\frac{t'}{N}\sum_{\substack{\mathbf{k},\mathbf{k}'\\ \mathbf{J},\alpha}}\Big(\chi^f_{(\mathbf{J}+\mathbf{a}_1+\mathbf{a}_2)\alpha J\alpha}\mathrm{e}^{-i\mathbf{J}\cdot(\mathbf{k}-\mathbf{k}')}\mathrm{e}^{i\mathbf{k}\cdot(\mathbf{a}_1+\mathbf{a}_2)}X^*_{\mathbf{k}\alpha}X_{\mathbf{k}'\alpha} \\ &+\chi^f_{(\mathbf{J}+\mathbf{a}_2)BJA}\mathrm{e}^{-i\mathbf{J}(\mathbf{k}-\mathbf{k}')}\mathrm{e}^{-i\mathbf{k}\cdot\mathbf{a}_2}X^*_{\mathbf{k}\alpha}X_{\mathbf{k}'\alpha}+\chi^f_{(\mathbf{J}-\mathbf{a}_1)\alpha J\alpha}\mathrm{e}^{-i\mathbf{J}\cdot(\mathbf{k}-\mathbf{k}')}\mathrm{e}^{i\mathbf{k}\cdot\mathbf{a}_1}X^*_{\mathbf{k}\alpha}X_{\mathbf{k}'\alpha}+h.c\Big)\ . \end{aligned} \tag{A.4}$$

In order to use the delta function we need to make an ansatz for the order parameters. Within the dimer ansatz the Hamiltonian becomes

$$\begin{aligned} H &= -t\sum_{\mathbf{k}}\Big(\Big[\chi^f_1+\chi^f_2\left(\mathrm{e}^{-i\mathbf{k}\cdot\mathbf{a}_2}+\mathrm{e}^{i\mathbf{k}\cdot\mathbf{a}_1}\right)\Big]X^*_{\mathbf{k}B}X_{\mathbf{k}A}+h.c\Big) \\ &-t'\sum_{\mathbf{k},\alpha}\Big(\Big[\chi^{f}_{1}{}'\mathrm{e}^{-i\mathbf{k}\cdot(\mathbf{a}_1+\mathbf{a}_2)}+\chi^{f}_{2}{}'\left(\mathrm{e}^{-i\mathbf{k}\cdot\mathbf{a}_2}+\mathrm{e}^{i\mathbf{k}\cdot a_1}\right)\Big]X^*_{\mathbf{k}\alpha}X_{\mathbf{k}\alpha}+h.c\Big)\,. \end{aligned} \tag{A.5}$$

If we define

$$\Omega^f_{\mathbf{k}}\equiv\chi^f_1+\chi^f_2\left(\mathrm{e}^{-i\mathbf{k}\cdot\mathbf{a}_2}+\mathrm{e}^{i\mathbf{k}\cdot\cdot\mathbf{a}_1}\right) \tag{A.6}$$

and

$$\Gamma^f_{\mathbf{k}}\equiv 2\left(\chi^{f}_{1}{}'\cos[\mathbf{k}\cdot(\mathbf{a}_1+\mathbf{a}_2)]+\chi^{f}_{2}{}'[\cos(\mathbf{k}\cdot\mathbf{a}_2)+\cos(\mathbf{k}\cdot\mathbf{a}_1)]\right)\ , \tag{A.7}$$

we can write the above Hamiltonian in matrix form as

$$H=\sum_{\mathbf{k}}(X^*_{\mathbf{k}A}\ \ X^*_{\mathbf{k}B})\begin{pmatrix}-t'\Gamma^f_{\mathbf{k}} & -t\Omega^{f*}_{\mathbf{k}}\\ -t\Omega^f_{\mathbf{k}} & -t'\Gamma^f_{\mathbf{k}}\end{pmatrix}\begin{pmatrix}X_{\mathbf{k}A}\\ X_{\mathbf{k}B}\end{pmatrix}\ . \tag{A.8}$$

This gives the spectrum, obtained by diagonalizing the matrix above, as

$$e^X_s(\mathbf{k})=-t'\Gamma^f_{\mathbf{k}}+st\sqrt{|\Omega^f_{\mathbf{k}}|^2}\ , \tag{A.9}$$

where s is the band index.

The calculation for the fermion spectrum is identical to the boson calculation up to

the changes $t' \to t' e^{i\phi_{ijc}}$, $X_i \to f_i$, and $\chi^f_{ij} \to \chi^X_{ij}$. The fermion Hamiltonian is given by

$$\begin{aligned} H &= -\frac{t}{N}\sum_{\substack{\mathbf{k},\mathbf{k}',\mathbf{J}\\ \sigma,a}} \Big(\chi^X_{\mathbf{J}BJA} e^{-i\mathbf{J}\cdot(\mathbf{k}-\mathbf{k}')} f^*_{\mathbf{k}Ba\sigma} f_{\mathbf{k}'Aa\sigma} + \chi^X_{(\mathbf{J}+a_2)BJA} e^{-i\mathbf{J}\cdot(\mathbf{k}-\mathbf{k}')} e^{-i\mathbf{k}\cdot\mathbf{a}_2} f^*_{\mathbf{k}Ba\sigma} f_{\mathbf{k}'Aa\sigma} \\ &\qquad + \chi^X_{(\mathbf{J}-\mathbf{a}_1)BJA} e^{-i\mathbf{J}\cdot(\mathbf{k}-\mathbf{k}')} e^{i\mathbf{k}\cdot\mathbf{a}_1} f^*_{\mathbf{k}Ba\sigma} f_{\mathbf{k}'Aa\sigma} + h.c\Big) \\ &\quad -\frac{t'}{N}\sum_{\substack{\mathbf{k},\mathbf{k}',\mathbf{J}\\ \sigma,\alpha}} \Big(\chi^X_{(\mathbf{J}+\mathbf{a}_1+\mathbf{a}_2)\alpha\mathbf{J}\alpha} e^{-i\mathbf{J}\cdot(\mathbf{k}-\mathbf{k}')} e^{i\mathbf{k}\cdot(\mathbf{a}_1+\mathbf{a}_2)+i\phi_{ij}\sigma} f^*_{\mathbf{k}\alpha 1\sigma} f_{\mathbf{k}'\alpha 1\sigma} \\ &\qquad + \chi^X_{(\mathbf{J}+\mathbf{a}_2)BJA} e^{-i\mathbf{J}\cdot(\mathbf{k}-\mathbf{k}')} e^{-i\mathbf{k}\cdot\mathbf{a}_2+i\phi_{ij}\sigma} f^*_{\mathbf{k}\alpha 1\sigma} f_{\mathbf{k}'\alpha 1\sigma} \\ &\qquad + \chi^X_{(\mathbf{J}-\mathbf{a}_1)\alpha\mathbf{J}\alpha} e^{-i\mathbf{J}\cdot(\mathbf{k}-\mathbf{k}')} e^{i\mathbf{k}\cdot\mathbf{a}_1+i\phi_{ij}\sigma} f^*_{\mathbf{k}\alpha 1\sigma} f_{\mathbf{k}'\alpha 1\sigma} + h.c\Big) \ . \end{aligned} \tag{A.10}$$

Here we again choose the dimer ansatz as we did in the boson case. There is one subtlety here that did not appear in the bosonic case. The spin dependent phase in the next nearest neighbour hopping terms must be chosen. We will use the convention of Haldane [37]. We assign a positive phase, $e^{i\phi}$, if a spin hops around the honeycomb in the clock-wise direction and a negative phase, $e^{-i\phi}$, if it hops in the counter clock-wise direction. With this convention we have the phases for each order parameter as

$$\begin{aligned} \phi_{A_{\mathbf{J}+\mathbf{a}_1+\mathbf{a}_2}A_{\mathbf{J}}} &= +\phi, \quad \phi_{B_{\mathbf{J}+\mathbf{a}_1+\mathbf{a}_2}B_{\mathbf{J}}} = -\phi \\ \phi_{A_{\mathbf{J}+\mathbf{a}_2}A_{\mathbf{J}}} &= -\phi, \quad \phi_{B_{\mathbf{J}+\mathbf{a}_2}B_{\mathbf{J}}} = +\phi \\ \phi_{A_{\mathbf{J}-\mathbf{a}_1}A_{\mathbf{J}}} &= +\phi, \quad \phi_{B_{\mathbf{J}-\mathbf{a}_1}B_{\mathbf{J}}} = -\phi \end{aligned}$$

. We then proceed in the same manner as above to arrive at the spectrum for the spinons

$$\begin{aligned} e^f_{sa\sigma}(\mathbf{k}) = -\frac{t'}{2}\delta_{a1}\left[A_\sigma(\mathbf{k},\phi) + B_\sigma(\mathbf{k},\phi)\right] + \frac{s}{2}\Big\{\Big[t'\left(A_\sigma(\mathbf{k},\phi) + B_\sigma(\mathbf{k},\phi)\right)\Big]^2\delta_{a1} \\ -4\left[(t')^2 A_\sigma(\mathbf{k},\phi)B_\sigma(\mathbf{k},\phi)\delta_{a1} - t^2|\Omega^X_{\mathbf{k}}|^2\right]\Big\}^{1/2} \end{aligned} \tag{A.11}$$

where the functions, $\Omega^X_{\mathbf{k}}$, $A_\sigma(\mathbf{k},\phi)$, and $B_\sigma(\mathbf{k},\phi)$ are defined as

$$\begin{aligned} \Omega^X_{\mathbf{k}} &= \chi^X_1 + \chi^X_2\left[e^{-i\mathbf{k}\cdot\mathbf{a}_2} + e^{i\mathbf{k}\cdot\mathbf{a}_1}\right] \\ A_\sigma(\mathbf{k},\phi) &= 2\chi^{X'}_1\cos(\mathbf{k}\cdot[\mathbf{a}_1+\mathbf{a}_2] - \sigma\phi) + 2\chi^{X'}_2[\cos(\mathbf{k}\cdot\mathbf{a}_2 + \sigma\phi) + \cos(\mathbf{k}\cdot\mathbf{a}_1 + \sigma\phi)] \\ B_\sigma(\mathbf{k},\phi) &= 2\chi^{X'}_1\cos(\mathbf{k}\cdot[\mathbf{a}_1+\mathbf{a}_2] + \sigma\phi) + 2\chi^{X'}_2[\cos(\mathbf{k}\cdot\mathbf{a}_2 - \sigma\phi) + \cos(\mathbf{k}\cdot\mathbf{a}_1 - \sigma\phi)] \end{aligned} \tag{A.12}$$

Appendix B

Bose Condensation

In this section we will compute the Bose condensation amplitude for the free boson fields X_i. We may accomplish this task by considering the two body boson correlation function in real space

$$\langle X^*_{\alpha,\mathbf{r}_i}(\tau) X_{\alpha,\mathbf{r}_j}(\tau')\rangle = \frac{1}{\mathcal{Z}} \int \mathcal{D}X\mathcal{D}X^* \left[X^*_{\alpha,\mathbf{r}_i}(\tau) X_{\alpha,\mathbf{r}_j}(\tau')\right] \mathrm{e}^{-\int d\tau L}, \tag{B.1}$$

where the index $\alpha = A, B$ refers to the sublattice and $\mathbf{r}_i$ the position vectors of the Brillouin zone. The Bose condensation amplitude is defined through the equal time correlation function as

$$Z \equiv \lim_{\Delta\mathbf{r}\to\infty} \sqrt{\langle X^*_{\alpha,\mathbf{r}_i}(\tau) X_{\alpha,\mathbf{r}_j}(\tau)\rangle}, \tag{B.2}$$

where $|\Delta\mathbf{r}| = |\mathbf{r}_i - \mathbf{r}_j|$. Transforming to momentum space equation B.1 becomes

$$\langle X^*_{\alpha,\mathbf{r}_i}(\tau) X_{\alpha,\mathbf{r}_j}(\tau')\rangle = \frac{1}{N} \sum_{\substack{\mathbf{k},\mathbf{k}' \\ \omega,\omega'}} \mathrm{e}^{-i\omega\tau + i\omega'\tau'} \mathrm{e}^{i\mathbf{k}\cdot\mathbf{r}_i - i\mathbf{k}'\cdot\mathbf{r}_j} \langle X^*_{\alpha,\mathbf{k}}(\omega) X_{\alpha,\mathbf{k}'}(\omega')\rangle. \tag{B.3}$$

In momentum space the average $\langle ... \rangle$ is computed with the boson action

$$S^X = \sum_{\substack{\mathbf{k},\omega \\ s}} \left\{ \frac{1}{4U}[-\omega + i\bar{h}_+]^2 + \mathrm{e}^X_s(\mathbf{k}) - \bar{\lambda} \right\} |X_s(\mathbf{k},\omega)|^2, \tag{B.4}$$

where $s = \pm$ is the band index and the new eigenfields may be defined by

$$\begin{bmatrix} X_+ \\ X_- \end{bmatrix} = \begin{bmatrix} -\frac{\Omega^*(\mathbf{k})}{|\Omega(\mathbf{k})|}(X_A - X_B) \\ X_A + X_B \end{bmatrix}. \tag{B.5}$$

The function $\Omega(\mathbf{k})$ is defined in appendix A.

With these fields the momentum space average becomes

$$\begin{aligned}\langle X^*_{\alpha,\mathbf{r}_i}(\tau)X_{\alpha,\mathbf{r}_j}(\tau')\rangle &= \frac{1}{4N}\frac{1}{\mathcal{Z}}\sum_{\substack{\mathbf{k},\mathbf{k}'\\ \omega,\omega'}} \mathrm{e}^{-i\omega\tau\,+\,i\omega'\tau'}\,\mathrm{e}^{i\mathbf{k}\cdot\mathbf{r}_i-\,i\mathbf{k}'\cdot\mathbf{r}_j} \\ &\times \int \mathcal{D}X_+\mathcal{D}X_-\left(X^*_{-1}X_{-1}+X^*_{+1}X_{+1}\right)\mathrm{e}^{-\sum_{\mathbf{k},\omega,s}X^*_{s,\mathbf{k}}(\omega)\ \mathbf{M}\ X_{s,\mathbf{k}}(\omega)},\end{aligned} \tag{B.6}$$

where $\mathbf{M}$ is the matrix representation of the operator in equation (B.4) and we have ignored cross terms between the (+) and (-) flavours since the integral will evaluate to zero for such terms. Upon performing this Gaussian integration over the Bose fields we have

$$\begin{aligned}\langle X^*_{\alpha,\mathbf{r}_i}(\tau)X_{\alpha,\mathbf{r}_j}(\tau')\rangle &= \frac{1}{4N}\sum_{\substack{\mathbf{k},\mathbf{k}'\\ \omega,\omega'}} \mathrm{e}^{\,-i\omega\tau\,+\,i\omega'\tau'}\,\mathrm{e}^{\,i\mathbf{k}\cdot\mathbf{r}_i-\,i\mathbf{k}'\cdot\mathbf{r}_j}\delta_{\mathbf{k},\mathbf{k}'}\delta_{\omega,\omega'} \\ &\times\left([\mathbf{M}]^{-1}_{(-1,\mathbf{k},\omega);(-1,\mathbf{k}',\omega')}+[\mathbf{M}]^{-1}_{(+1,\mathbf{k},\omega);(+1,\mathbf{k}',\omega')}\right) \\ &= \frac{1}{4N}\sum_{\mathbf{k},\omega}\mathrm{e}^{\,-i\omega(\tau-\tau')}\mathrm{e}^{\,i\mathbf{k}\cdot(\mathbf{r}_i-\mathbf{r}_j)} \\ &\times\left([\mathbf{M}]^{-1}_{(-1,\mathbf{k},\omega);(-1,\mathbf{k}\cdot\omega)}+[\mathbf{M}]^{-1}_{(+1,\mathbf{k},\omega);(+1,\mathbf{k},\omega)}\right) \\ &= \frac{1}{4N}\sum_{\mathbf{k},\omega}\mathrm{e}^{\,-i\omega(\tau-\tau')}\mathrm{e}^{\,i\mathbf{k}\cdot(\mathbf{r}_i-\mathbf{r}_j)} \\ &\left(\frac{4U}{(-\omega+ih_+)^2+4U(\mathrm{e}^X_{-1}(\mathbf{k})-\lambda)}\right. \\ &\qquad\left.+\frac{4U}{(-\omega+ih_+)^2+4U(\mathrm{e}^X_{+1}(\mathbf{k})-\lambda)}\right).\end{aligned} \tag{B.7}$$

Now that we have an expression for the correlation function we can compute the Bose condensation amplitude (B.2) as

$$\begin{aligned}Z^2 &= \lim_{\Delta\mathbf{r}\to\infty}\frac{1}{4N}\sum_{\mathbf{k},\omega}\mathrm{e}^{\,i\mathbf{k}\cdot(\mathbf{r}_i-\mathbf{r}_j)} \\ &\times\left(\frac{4U}{(-\omega+ih_+)^2+4U(\mathrm{e}^X_{-1}(\mathbf{k})-\lambda)}+\frac{4U}{(-\omega+ih_+)^2+4U(\mathrm{e}^X_{+1}(\mathbf{k})-\lambda)}\right)\end{aligned}$$

$$= \frac{1}{4N}\sum_{\omega}\left(\frac{4U}{(-\omega+ih_+)^2+4U(\mathrm{e}^X_{-1}(0)-\lambda)}+\frac{4U}{(-\omega+ih_+)^2+4U(\mathrm{e}^X_{+1}(0)-\lambda)}\right). \quad \text{(B.8)}$$

In the zero temperature limit this sum becomes an integral over the continuous frequency

$$Z^2 = \frac{1}{4N}\int\frac{d\omega}{2\pi}\left(\frac{4U}{(-\omega+ih_+)^2+4U(\mathrm{e}^X_{-1}(0)-\lambda)} + \frac{4U}{(-\omega+ih_+)^2+4U(\mathrm{e}^X_{+1}(0)-\lambda)}\right). \quad \text{(B.9)}$$

Integrals of this type are well documented and may easily be performed [38]. Thus we arrive at the Bose condensation amplitude

$$Z^2 = \frac{1}{8N}\left(\sqrt{\frac{4U}{(\mathrm{e}^X_{-1}(0)-\lambda)}}+\sqrt{\frac{4U}{(\mathrm{e}^X_{+1}(0)-\lambda)}}\right). \quad \text{(B.10)}$$

In the thermodynamic limit the chemical potential of the bosons becomes $\lambda = \mathrm{e}^X_{-1}(0)$. Thus when we take $N \to \infty$ the only term that remains finite is the first term, which gives

$$Z^2 = \frac{1}{8N}\sqrt{\frac{4U}{(\mathrm{e}^X_{-1}(0)-\lambda)}}. \quad \text{(B.11)}$$

Appendix C

Fermionic Coherent States

Definition 1. *Two numbers, α and β, are said to be Grassmann numbers if they satisfy the property $\alpha\beta = -\beta\alpha$. In other words, they satisfy the algebra*

$$\{\alpha, \beta\} = 0 \qquad \{\alpha, \alpha\} = 0 \qquad \{\beta, \beta\} = 0$$

where $\{A, B\} = AB + BA$.

We can use these numbers to define a set fermionic coherent states by satisfying the relations[1]

$$\{\alpha_i, c_j\} = 0 \qquad\qquad (\alpha_i c_i)^\dagger = c_j^\dagger \bar{\alpha}_i \tag{C.1}$$

where c_j is a electronic destruction operator. Once equation (C.1) is satisfied we may write down the coherent states as

$$|\alpha\rangle = \mathrm{e}^{-\sum_i \alpha_i c_i^\dagger}|0\rangle \tag{C.2}$$

where $|0\rangle$ is the vacuum state with no fermions. It is straightforward to show that this is indeed a coherent state by expanding the exponential as a power series, which gives the result

$$c_j|\alpha\rangle = \alpha_j|\alpha\rangle \ .$$

With this definitions of the coherent states we can derive the completeness and closure

[1]Notice that the number $\bar{\alpha}$ is NOT the same as the complex conjugate. This is due to the fact that the Grassmann algebra is an exterior alegebra, so we must treat this number as independent of α.

relations for these states as

$$\begin{aligned} \langle\beta|\alpha\rangle &= \mathrm{e}^{\sum_i \bar{\beta}_i \alpha_i} \\ \mathbf{I}_f &= \int d(\bar{\alpha}, \alpha) \mathrm{e}^{-\sum_i \bar{\alpha}_i \alpha_i} |\alpha\rangle\langle\alpha| \end{aligned} \tag{C.3}$$

where $d(\bar{\alpha}, \alpha) = \prod_i d\bar{\alpha}_i d\alpha_i$.

Appendix D

Coherent States of Angular Momentum

Consider some operator $n_{i\alpha}$, that has an infinite set of integral eigenvalues, which is canonically conjugate to the phase operator θ_i^α namely

$$[n_{i\alpha}, \theta_j^\beta] = i\delta_{ij}\delta_{\alpha\beta} \ . \tag{D.1}$$

With this algebra we may then expand the eigenstates of the phase operator, $|\theta_i^\alpha\rangle$, as

$$|\theta_i^\alpha\rangle = \sum_{n_{i\alpha}=-\infty}^{\infty} \mathrm{e}^{in_{i\alpha}\theta_i^\alpha} |n_{i\alpha}\rangle \ . \tag{D.2}$$

It is then straightforward to check that the inner product between two θ states obeys

$$\langle \theta_i^\alpha | \theta_j^{\beta'} \rangle = 2\pi\delta_{ij}\delta_{\alpha\beta}\delta(\theta - \theta') \ . \tag{D.3}$$

Using these relations we may then write down the $n_{i\alpha}$ states in the θ_i^α representation as

$$|n_{i\alpha}\rangle = \int_0^{2\pi} \frac{d\theta_i^\alpha}{2\pi} \mathrm{e}^{-in_{i\alpha}\theta_i^\alpha} |\theta_i^\alpha\rangle \ . \tag{D.4}$$

With these properties we can now write down the overlap of the two representations as

$$\langle n_{i\alpha} | \theta_i^\alpha \rangle = \mathrm{e}^{in_{i\alpha}\theta_i^\alpha} \ . \tag{D.5}$$

Bibliography

[1] C. L. Kane and E. J. Mele. Quantum spin hall effect in graphene. *Phys. Rev. Lett.*, **95**:226801, (2005).

[2] B. Andrei Bernevig and Shou-Cheng Zhang. Quantum spin hall effect. *Phys. Rev. Lett.*, **96**:106802, (2006).

[3] C. L. Kane and E. J. Mele. $\mathbb{Z}_2$ topological order and the quantum spin hall effect. *Phys. Rev. Lett.*, **95**:146802, (2005).

[4] Rahul Roy. Three dimensional topological invariants for time reversal invariant hamiltonians and the three dimensional quantum spin hall effect. *arXiv.org:cond-mat/0607531*, (2006).

[5] J. E. Moore and L. Balents. Topological invariants of time-reversal-invariant band structures. *Phys. Rev. B*, **75**:121306, (2007).

[6] Liang Fu, C. L. Kane, and E. J. Mele. Topological insulators in three dimensions. *Phys. Rev.Lett.*, **98**:106803, (2007).

[7] Yugui Yao, Fei Ye, Xiao-Liang Qi, Shou-Cheng Zhang, and Zhong Fang. Spin-orbit gap of graphene: First-principles calculations. *Phys. Rev. B*, **75**:041401, (2007).

[8] B. Andrei Bernevig, Taylor L. Hughes, and Shou-Cheng Zhang. Quantum Spin Hall Effect and Topological Phase Transition in HgTe Quantum Wells. *Science*, **314**:1757–1761, (2006).

[9] Markus Konig, Steffen Wiedmann, Christoph Brune, Andreas Roth, Hartmut Buhmann, Laurens W. Molenkamp, Xiao-Liang Qi, and Shou-Cheng Zhang. Quantum Spin Hall Insulator State in HgTe Quantum Wells. *Science*, **318**:766–770, (2007).

[10] Congjun Wu, B. Andrei Bernevig, and Shou-Cheng Zhang. Helical liquid and the edge of quantum spin hall systems. *Phys. Rev. Lett.*, **96**:106401, (2006).

[11] Cenke Xu and J. E. Moore. Stability of the quantum spin hall effect: Effects of interactions, disorder, and $\mathbb{Z}_2$ topology. *Phys. Rev. B*, **73**:045322, (2006).

[12] Andrew M. Essin and J. E. Moore. Topological insulators beyond the brillouin zone via chern parity. *Phys. Rev. B*, **76**:165307, (2007).

[13] Sung-Sik Lee and Shinsei Ryu. Many-body generalization of the $\mathbb{Z}_2$ topological invariant for the quantum spin hall effect. *Phy. Rev. Lett.*, **100**:186807, (2008).

[14] X.-L. Qi and S.-C. Zhang. Spin charge separation in the quantum spin hall state. *arXiv:0801.0252*, (2008).

[15] A. Vishwanath Y. Ran and D.-H. Lee. Spin-charge separated solitons in a topological band insulator. *arXiv:0801.0627*, (2008).

[16] S. Raghu, X.-L. Qi, C. Honerkamp, and S.-C. Zhang. Topological mott insulators. *arXiv:0710.0030*, (2007).

[17] Tarun Grover and T. Senthil. Topological spin hall states, charged skyrmions, and superconductivity in two dimensions. *Phys. Rev. Lett.*, **100**:156804, (2008).

[18] P. W. Anderson. The Resonating Valence Bond State in La2CuO4 and Superconductivity. *Science*, **235**:1196–1198, (1987).

[19] P. Fazekas and P. W. Anderson. On the ground state properties of the anisotropic triangular antiferromagnet. (application of anisotropic heisenberg model). *Philos. Mag.*, **30**:423–440, (1974).

[20] Patrick A. Lee, Naoto Nagaosa, and Xiao-Gang Wen. Doping a mott insulator: Physics of high-temperature superconductivity. *Rev. Mod. Phys.*, **78**:17, (2006).

[21] Xiao-Gang Wen. Quantum orders and symmetric spin liquids. *Phys. Rev. B*, **65**:165113, Apr (2002).

[22] Y. Shimizu, K. Miyagawa, K. Kanoda, M. Maesato, and G. Saito. Spin liquid state in an organic mott insulator with a triangular lattice. *Phys. Rev. Lett.*, **91**:107001, Sep (2003).

[23] J. S. Helton, K. Matan, M. P. Shores, E. A. Nytko, B. M. Bartlett, Y. Yoshida, Y. Takano, A. Suslov, Y. Qiu, J.-H. Chung, D. G. Nocera, and Y. S. Lee. Spin dynamics of the spin-1/2 kagome lattice antiferromagnet $ZnCu_3(OH)_6Cl_2$. *Phys. Rev. Lett.*, **98**:107204, (2007).

[24] Sung-Sik Lee and Patrick A. Lee. U(1) gauge theory of the hubbard model: Spin liquid states and possible application to κ-$(BEDT\text{-}TTF)_2Cu_2(CN)_3$. *Phys. Rev. Lett.*, **95**:036403, (2005).

[25] Michael Hermele. Su(2) gauge theory of the hubbard model and application to the honeycomb lattice. *Phys. Rev. B*, **76**:035125, (2007).

[26] A.M. Polyakov. Compact gauge fields and the infrared catastrophe. *Phys. Lett. B*, **59**:82–84, October (1975).

[27] Serge Florens and Antoine Georges. Slave-rotor mean-field theories of strongly correlated systems and the mott transitionin finite dimensions. *Phys. Rev. B*, **70**:035114, Jul (2004).

[28] E. Fradkin. *Field Theories of Condensed Matter.* Perseus Books, (1991).

[29] N. D. Mermin and H. Wagner. Absence of ferromagnetism or antiferromagnetism in one- or two-dimensional isotropic heisenberg models. *Phys. Rev. Lett.*, **17**:1133–1136, Nov (1966).

[30] Ian Affleck and J. Brad Marston. Large-n limit of the heisenberg-hubbard model: Implications for high-*tc* superconductors. *Phys. Rev. B*, **37**:3774–3777, Mar (1988).

[31] B. Simons A. Altland. *Condensed Matter Field Theory.* Cambridge University Press, (2006).

[32] W.H. Press *et al.* *Numerical Recipes in C.* Cambridge University Press, second edition, (1992).

[33] R.B. Laughlin. Quantized hall conductivity in two dimensions. *Phys. Rev. B*, **23**:5632–5633, May (1981).

[34] J.Schwinger. Gauge invariance and mass. *Phys. Rev.*, **125**:397–398, (1962).

[35] John B. Kogut. An introduction to lattice gauge theory and spin systems. *Rev. Mod. Phys.*, **51**:659–713, Oct (1979).

[36] Franz J. Wegner. Duality in generalized ising models and phase transitions without local order parameters. *J. Math. Phys.*, **12**:2259–2272, (1971).

[37] F. D. M. Haldane. Model for a quantum hall effect without landau levels: Condensed-matter realization of the parity anomaly. *Phys. Rev. Lett.*, **61**:2015–2018, Oct (1988).

[38] M. J. Marsden J. E. Hoffman. *Basic Complex Analysis.* W. H. Freeman and Company, (1987).